SPATIOTEMPORAL AND DIRECTIONAL PROPERTIES OF VISUAL NEURONS IN THE LENTIFORMIS MESENCEPHALI OF THE ZEBRA FINCH AND HUMMINGBIRD

by

Graham Smyth

B.Sc., University of Ottawa, April 2016

A THESIS SUBMITTED IN PARTIAL FULFILLMENT OF THE REQUIREMENTS

FOR THE DEGREE OF

MASTER OF SCIENCE

in

THE FACULTY OF GRADUATE AND POSTDOCTORAL STUDIES

(Zoology)

The University of British Columbia

(Vancouver)

July 2018

The following individuals certify that they have read, and recommend to the Faculty of Graduate and Postdoctoral Studies for acceptance, a thesis/dissertation entitled:

Spatiotemporal and directional properties of visual neurons in the lentiformis mesencephali of the zebra finch and hummingbird

submitted by Graham C. Smyth in partial fulfillment of the requirements for

the degree of Master of Science

in Zoology

Examining Committee:

Douglas Altshuler
Supervisor

Michael Gordon
Supervisory Committee Member

James Enns
Supervisory Committee Member

William Milsom
External Examiner

Abstract

A moving animal experiences global visual signals across the entire retina known as optic flow, one of the key signals used in visual guidance of locomotion. Optic flow sensitive neurons have been identified in the midbrains of all vertebrate classes. In birds, these neurons are found in the nucleus of the basal optic root (nBOR) and the pretectal nucleus lentiformis mesencephali (LM). These cells are known to exhibit large receptive fields in the contralateral eye, are excited by visual motion in a "preferred" direction and are inhibited by motion in the opposite direction. A key question is whether the response properties of LM neurons are conserved across species or are LM neurons specialized in animals that use different locomotor strategies. Previous studies in pigeons have investigated the responses of neurons in the LM and nBOR to drifting sine-wave gratings and discovered that they are tuned in the spatiotemporal domain. The LM typically contains cells that respond maximally to fast stimuli and are tuned to temporal frequency whereas nBOR cells respond maximally to slower stimuli and are velocity-tuned. Here we ask whether zebra finches and hummingbirds, specialized for different modes of locomotion, exhibit spatiotemporal specializations in optic flow neurons that may be related to their form of locomotion. We explored this question by making extracellular recordings in the LM of anesthetized birds while presenting drifting sine-wave gratings to the contralateral eye. These results were compared with previous pigeon data and we found that each of the three species exhibits distinct tuning in the spatiotemporal domain. Hummingbird LM neurons are tuned to the fastest stimuli, which were typically of lower spatial frequencies. Both hummingbird and finch LM cells exist almost exclusively as fast cells with 90% of peaks in the fast zone. Moreover, in pigeons, only 'slow' cells are velocity tuned, whereas both zebra finches and hummingbirds have

‘fast’ cells that are velocity tuned. These species-specific differences are suggestive of neural specializations for different optic flow behavior.

Lay Summary

Optic flow—global image motion resulting from self-motion—is a visual signal that is critical for controlling locomotion. Optic flow processing begins with large-field motion detectors in the midbrain. We focus on optic flow processing in birds because their visual circuits are extensive, well-described, and highly conserved with mammals. A key question is whether the response properties of optic flow neurons are conserved across species or are they specialized for different locomotor strategies. We presented sine wave gratings of varying spatial and temporal frequencies while making extracellular recordings from neurons in zebra finches (*Taeniopygia guttata*) and Anna's hummingbirds (*Calypte anna*). Comparing new data from zebra finches and hummingbirds with previously published data from pigeons revealed that the three species have optic flow neurons with distinct spatiotemporal tuning properties. These species-specific differences are suggestive of neural specializations for different behavior.

Preface

All of the work presented in this thesis was conducted in the Altshuler laboratory at the University of British Columbia, Vancouver campus. This is apart from the anatomical analysis in section 2.3.4 which was conducted in the Wylie laboratory at the University of Alberta in Edmonton, Alberta.

The research in Chapter 2 of this thesis is original and unpublished. This project was inspired partly by a previous study considering the spatiotemporal tuning of LM neurons carried out in pigeons in 2003 by Wylie et al. The experimental design and stimuli used by Wylie et al. 2003 influenced that of the current study, however considerable effort was made to use the most current methods for completing experiments. All surgical, electrophysiological, and histological protocols were carried out by myself with initial assistance and training from Dr. Andrea Gaede.

I was responsible for performing all surgeries, collecting all electrophysiological data from the animal subjects, and analyzing all electrophysiological data. All visual stimuli used in experiments were modified from previous MATLAB code created by Dr. Benny Goller. Spike sorting using spike2 software was completed offline after experiments.

All experimental procedures were approved by the UBC Animal Care Committee and conducted in accordance with guidelines set forth by the Canadian Council on Animal Care.

Throughout the entirety of the degree, I received guidance from my supervisor Dr. Douglas Altshuler and my supervisory committee members, Dr. Michael Gordon and Dr. James Enns.

Table of Contents

List of Tables

List of Figures

List of Abbreviations

AOS Accessory Optic System

LM Lentiformis Mesencephali

LML Lentiformis Mesencephali Pars Lateralis

LMM Lentiformis Mesencephali Pars Medialis

nBOR nucleus of the Basal Optic Root

SF Spatial frequency

TF Temporal Frequency

Acknowledgements

I would like to begin by thanking my supervisor Dr. Douglas Altshuler. Doug has been an incredible guide and mentor who has taught me valuable lessons through which I have grown immensely as a researcher and as a person. I wish you and your family all the best. My supervisory committee: Michael Gordon and Jim Enns, thank you for providing your valuable feedback and making committee meetings low-stress and fun. A very special thankyou to Dr. Andrea Gaede who has been contributed greatly to my scientific skill and knowledge. Dre taught me surgery, histology, electrophysiology and has helped me with almost every other aspect of research. Thank you to Dr. Douglas Wylie, and Cristian Gutierrez-Ibanez, my unofficial co-supervisors, for providing your knowledge and expertise and for being gracious hosts while I visited your lab in Edmonton. To my fellow lab mates, who have become close friends, you have always supported me and provided countless feedback throughout my degree. I wish you all the best in the future, I will miss you greatly.

Thank you to my parents, brother, and partner Monika for listening to presentations, correcting written work all while believing in me, giving me confidence through positive feedback, and maintaining my sanity during the stressful periods.

Lastly, thank you to the zoology department for providing a great environment to do science. The social nature of the department with events and gatherings along with the amazing research that I learned about through seminars and lectures is what makes this department outstanding.

1. Introduction

This thesis examines the visual response properties of neurons in the nucleus lentiformis mesencephali (LM), known to be key in processing visual motion related to self motion, in two bird species: the zebra finch and hummingbird. I will present this work by first reviewing the relevant literature broadly in the first introductory chapter. The second chapter will outline the methods and present the thesis results, and in the third and final chapter I will discuss my interpretation of the results in the context of previous research and suggest future directions and applications.

As we move through our environment, the objects, surfaces, and organisms which comprise our visual field move across our retina and create a signal of global visual motion that is known as *optic flow* (Gibson, 1954b, 1979). Optic flow can be visualized as a vector field in which every point in visual space has its own speed and direction of motion (Fig 1). Optic flow signals must be rapidly processed by the visual system to initiate and control motor programs during locomotion. This is especially important for flying animals that must navigate complex environments at high speed without the stability afforded by direct ground contact. It is unsurprising therefore, that flying animals tend to devote considerable neural resources to their visual systems. Birds for example have some of the largest eyes for a given body weight of any vertebrate (Howland et al., 2004; Kiltie, 2000) and exhibit enlarged optic-lobes (Vincze et al., 2015).

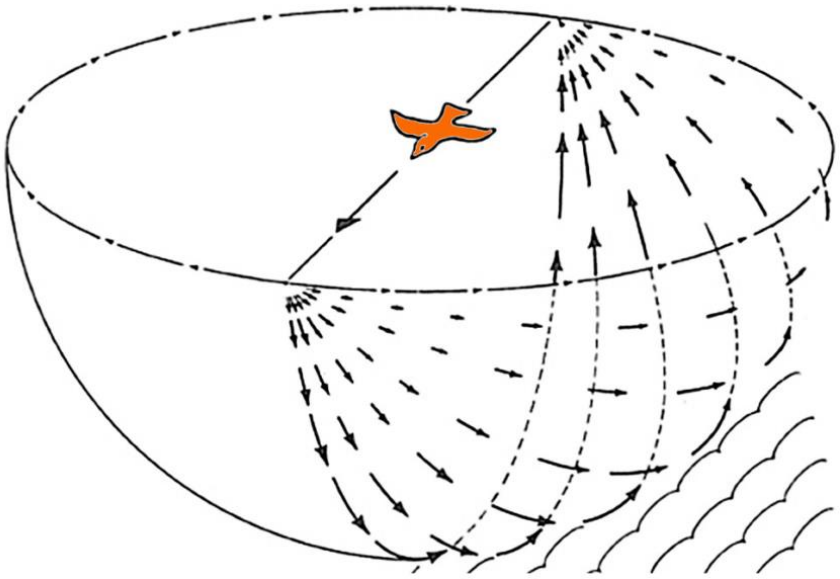

Figure 1. Optic flow during translational forward flight. During forward translation, the entire visual field moves across the retina to create optic flow. Every point in space has its own direction and speed of motion. Taken from Gibson, 1979.

Depending on the goal of a behaviour, certain visual algorithms or visual guidance strategies are employed to control aspects of flight such as position, altitude, speed, and orientation, which in-turn guide ecologically relevant behaviours such as predator-prey interaction. To understand how this can occur, it is helpful to consider the types of visual motion that are produced while an animal is in motion and how this can subserve motor control. A natural scene contains many complex patterns of light intensity changes from the very fine scale of lines in the bark of a tree, the intermediate scale of the tree trunk, all the way up to the large scale of a forest. The spatial frequency of a visual stimulus is defined as the number of cycles (wavelengths) of a light intensity change per degree of one's visual field. It is easier to visualize this concept if one considers a simple image such as a square wave grating (Fig 2). The number of wavelengths of a square wave that occur across one degree of visual field is the spatial frequency. When stimuli of a particular spatial frequency are moved in any direction, the time it takes for one cycle to move across one

point in space is the temporal frequency of that stimulus. Depending on the combination of spatial and temporal frequency of a stimulus, you get a particular pattern velocity of motion. This is because pattern velocity is the ratio of temporal frequency to spatial frequency. Motion sensitive neurons have been identified in animal visual systems which are tuned to one or a combination of spatial frequency, temporal frequency, or pattern velocity. What remains poorly understood is whether the spatiotemporal tuning of visual neurons is conserved across animals or are animals' visual systems specialized for their locomotor strategy? If specializations do exist, where in the visual system are they found? This thesis aims to test whether pigeons, zebra finches, and hummingbirds, birds that exhibit unique locomotor strategies, have spatiotemporal specializations in visual neurons. Furthermore, this thesis will determine whether the LM is the location where these specializations exist.

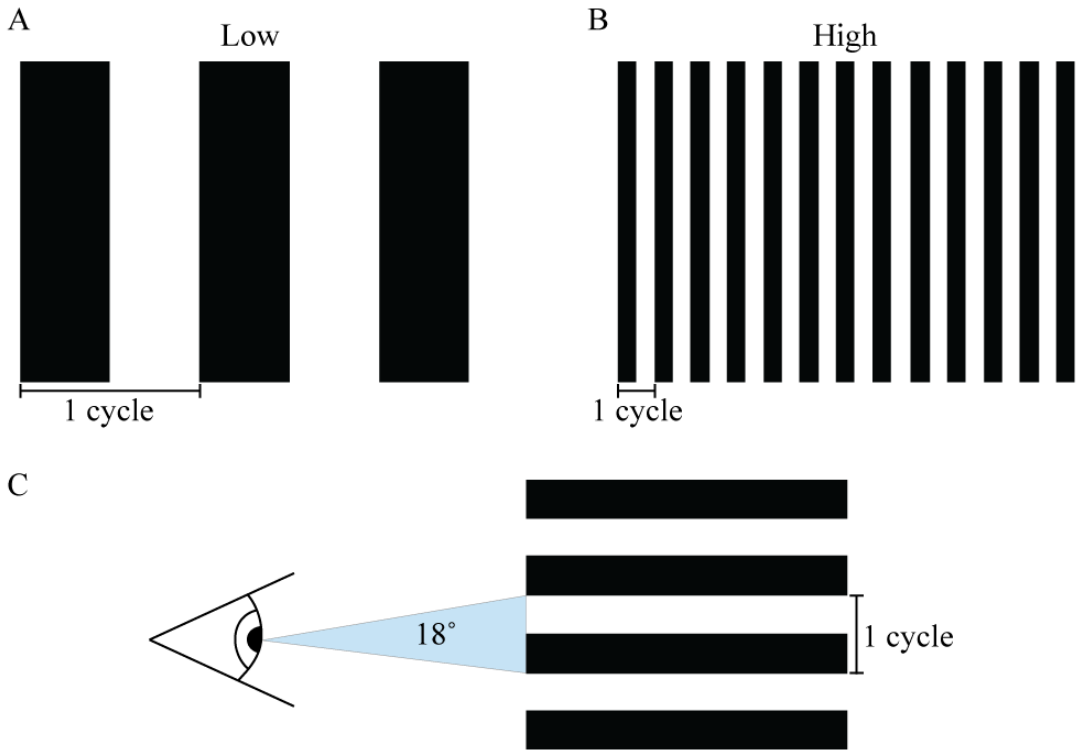

Figure 2. Spatial Frequency of Visual Stimuli. A) low spatial frequency square wave grating. B) high spatial frequency square wave grating. C) diagram illustrating how spatial frequency is measured in cycles per degree of visual field. The spatial frequency of this grating would be 1cycle/18° = 0.055 cycles per degree.

1.1 Visual Guidance of Flight in Insects

A visual guidance strategy is an algorithm or rule that an animal will use to control a specific aspect of locomotion in response to a specific visual stimulus. Our progress in understanding the visual guidance of flight has emerged mainly through studies of insects. Experimental investigations using virtual reality flight tunnels are common and provide a powerful system for revealing visual guidance strategies. As an insect flies down a tunnel, patterns can be projected on the tunnel walls and can be moved or manipulated during flight to provide an immersive virtual reality. Additionally, cameras can be placed above the tunnel to track the animal's motion. Flight tunnel studies using honeybees and fruit flies found that translational optic flow, optic flow resulting from translational motion, regulates flight speed (Baird et al., 2005; Fry et al., 2009). When translational optic flow is manipulated in either the forward or backward direction relative to the direction of flight, insects tend to adjust their flight speed such that the optic flow velocity is kept within a preferred range. One interpretation is that this strategy is an important mechanism for avoiding collision in cluttered environments. The closer one is to an object, the greater the optic flow signal for a given change in position. Thus, when a flying insect transitions from an open environment to a cluttered environment which creates a relatively increased optic flow input, flight speed will be decreased, and the chance of a high-speed collision is therefore reduced. Optic flow is also used to control vertical and horizontal flight position in *Drosophila melanogaster* (Straw et al., 2010) and in honeybees (Portelli et al., 2010). These animals control altitude based on optic flow in the ventral field and steer away from lateral field features which provide greater optic flow signals (Chakravarthi et al., 2017).

Behavioural (Goller & Altshuler, 2014) and electrophysiological (Gaede et al., 2017; Winterson & Brauth, 1985) experiments indicate that birds are also well equipped for processing

optic flow stimuli. What visual guidance strategies do birds use during locomotion and how do they differ from those used by insects?

1.2 The Visual Guidance of Flight in Birds

Possessing relatively complex nervous systems, birds may exhibit differences in visual guidance strategies compared to insects. Only a handful of studies have explored the visual guidance of bird flight; however, current results indicate that birds exhibit unique strategies for the visual guidance of flight speed compared to insects. Of the two species of birds used in these investigations, budgerigars and hummingbirds, unique strategies for controlling flight trajectory were found. These results raise the possibility that visual guidance may vary among bird species and potentially among flight mode specializations.

Two studies have explored the role of optic flow in flight speed regulation in budgerigars (Schiffner & Srinivasan, 2015, 2016). The researchers found that, like insects, when grating patterns were moved in the direction of flight, the budgies would increase flight speed relative to a static pattern but not enough to match the pattern-velocity of the grating as seen in insects. Additionally, when the gratings were moved in the opposite direction, flight speed was unaffected (Schiffner & Srinivasan, 2015). This shows that birds use optic flow to regulate flight-speed but there are other factors involved. Interestingly, similar experiments with hummingbirds showed that flight speed was not affected by optic flow manipulation (Roslyn Dakin, unpublished data). This not only suggests that insects and birds use different visual guidance strategies, but also that differences exist among bird species.

The visual guidance of hummingbird flight also differs from that of budgerigars in another important respect. When budgies fly through a tunnel with strong optic flow on one lateral wall

(vertical grating) and low or no optic flow on the other (either blank or horizontal grating), they steer towards the low optic flow wall (Bhagavatula et al., 2011). Hummingbirds are also known to exhibit this "centering" response; however, they do so only when gratings of specific spatial frequencies are presented (Dakin et al., 2016). Bhagavatula et al. only tested one spatial frequency (0.055 cycles per degree) and it therefore remains unknown whether the centering response in budgies is tuned to specific spatial frequencies. What we do know is that hummingbirds do not exhibit the centering response to gratings of the same spatial frequency (0.055 cpd) as budgies. Dakin et al. (2016) also tested the lateral position control of hummingbirds using horizontal gratings of different spatial frequencies on both lateral walls of a flight tunnel. Hummingbirds consistently steered towards the wall with the smaller horizontal gratings. This finding suggests that hummingbirds may be balancing the rate of vertical expansion of visual features to guide lateral position, rather than balancing pattern velocity (Altshuler & Srinivasan, 2018). Collectively, this suggests that at some level in the visual system, a difference exists in the spatial frequency tuning that influences the visual guidance of flight between budgerigars and hummingbirds. The observed behavioural differences may have evolved due to the unique optic flow stimuli associated with different flight modes. Hummingbirds can keep their head and beak stable during feeding bouts on the wing despite various environmental perturbations. We know that hummingbirds are highly sensitive to the direction and orientation of visual motion during hovering and will drift in response to minimal optic flow stimuli (Goller & Altshuler, 2014). The next section considers avian visual pathways and the neuroanatomical specializations that hummingbirds possess relative to other birds that may underlie their high optic flow sensitivity.

1.3 Visual Neuroanatomy

There are three visual pathways in the avian brain that process visual information from the environment: the tectofugal pathway, the thalamofugal pathway, and the accessory optic system. The tectofugal pathway is known to be involved in processing information related to color, whole field luminance, depth-related motion, and motion of small objects and edges (Wang et al., 1993). For these reasons, the tectofugal pathway has been generally associated with motion of objects in the environment rather than self-motion. The thalamofugal pathway is thought to be homologous to the geniculo-striate pathway (Retina – LGN – V1) in mammals (Medina & Reiner, 2000; Pettigrew & Konishi, 1976). The thalamofugal pathway has been implicated in visual motion perception such as the direction of motion (Baron et al., 2007) and in binocular vision (Pettigrew, 1978; Pettigrew & Konishi, 1976).

The final major visual pathway is the accessory optic system (AOS), a highly conserved pathway found in all vertebrate classes (Ibbotson & Price, 2001; McKenna & Wallman, 1985; Scalia, 1972; Simpson, 1984). The main function of this pathway is analyzing optic flow resulting from self-motion (Wylie & Crowder, 2000) but it also serves an important role in mediating gaze-stabilizing motor behaviours (Collewijn, 1975a; Collewijn, 1975b; Gioanni, 1988). The AOS begins with two midbrain nuclei known in birds as the nucleus of the basal optic root (nBOR) and the pretectal nucleus lentiformis mesencephali, which both receive direct retinal input (Wylie et al., 2014). The nBOR is homologous to the medial, and lateral terminal nuclei of the mammalian AOS and the LM is homologous to the mammalian pretectal nucleus of the optic tract (NOT) and dorsal terminal nucleus (DTN) (Fite, 1985; Ibbotson et al., 1994; McKenna & Wallman, 1985). There are extensive projections from the AOS to pre-motor structures including the inferior olive (Wylie, 2001) and folia VI through X of the cerebellum, which comprise the oculomotor

cerebellum and vestibulocerebellum (Gamlin, 2006; Gamlin & Cohen, 1988; Wylie et al., 2018). The LM and nBOR additionally receive considerable extra-retinal afferents from the telencephalon, ventral thalamus, and various mid-brain inputs including from the contralateral AOS (for review see Gamlin, 2006).

Studies in comparative anatomy of sensory systems have used relative size of sensory regions while considering allometry and phylogenetic history to explore the relationships between brain and behaviour (Iwaniuk & Wylie, 2007). Iwaniuk & Wylie (2007) conducted a comparative neuroanatomical study of 37 species of birds from 13 orders to determine whether hovering flight was associated with a change in the relative brain volume of visual nuclei. The researchers found hypertrophy in the LM of all hummingbird species studied where the average LM volume relative to brain volume in nine hummingbird species was approximately triple that of all non-hummingbird species measured. There were no other significant differences in any other visual nuclei studied including the nBOR and the optic tectum. The link between the enlargement of LM and hovering is further supported by the fact that the hummingbird LM was significantly larger than swifts and swiftlets, which have similar brain sizes and are closely related to hummingbirds. Species that are known to transiently hover such as the American kestrel, eastern spinebill, and belted kingfisher were all found to have significantly larger LM volumes compared to non-hovering species but were still significantly below the LM volume of hummingbirds. This strongly suggests a relationship between the relative size of LM and the visual environment experienced by birds which perform hovering flight. Indeed, because LM was selectively hypertrophied and other important visual areas were not, there may be an increased need for optic flow sensitivity in the hummingbird.

It is important to note that the LM should not be thought of as a homogenous structure as it is composed of two morphologically distinct subdivisions: the LM pars lateralis (LML) and the LM pars medialis (LMM), which also have unique connectivity and neurophysiology (Pakan et al., 2006). It has been suggested that in the hummingbird, these two regions are not hypertrophied uniformly (Wylie et al., 2018) but may be largely due to an expansion of the medial subdivision of the LM.

1.4 Neurophysiology of the AOS

Neurons in the LM and nBOR are characterized by several important traits that make them well-suited to analyzing optic flow stimuli. They exhibit large receptive fields on the order of 40°-150° in diameter, and prefer larger stimuli to smaller stimuli (Collewijn, 1975a; Winterson & Brauth, 1985; Wylie & Crowder, 2000). Their large receptive fields speak to the fact that many retinal fibers converge on single LM or nBOR cells (Ibbotson & Clifford, 2001; Wylie et al., 2014). These neurons are direction and velocity tuned to large-field stimuli that include dot-fields, sinusoidal gratings, and checkerboards. They exhibit increased activity to a preferred direction and velocity of image motion and are typically inhibited by motion in the opposite direction (Gaede et al., 2017; Wylie & Crowder, 2000) The quality of responding to large-field optic flow stimuli is unique with respect to other areas in the avian visual system as other motion responsive neurons respond to small object-like stimuli, and have large inhibitory surrounds resulting in an inability to respond to optic flow (Frost et al., 1990).

Although LM and nBOR are functionally similar they have distinct population-level direction preferences. The LM in almost every tetrapod studied has a strong bias for forward (temporo-nasal) visual motion including the cat (Hoffmann & Schoppmann, 1981), wallaby (Ibbotson et al., 1994), frog (Cochran et al., 1984), salamander (Manteuffel, 1982), primate

(Mustari & Fuchs, 1990) and bird (Gaede et al., 2017; Wylie & Crowder, 2000). The nBOR however, exhibits an overall preference for the other three cardinal directions (up, down, and backward or naso-temporal motion), which are represented equally in nBOR (Crowder, 2003; Ibbotson, 2017; Wylie & Frost, 1990). Interestingly, the hummingbird is the only animal studied to date where the LM doesn't seem to exhibit this forward-motion bias. Rather, at the population level, the hummingbird LM has a uniform distribution of direction preferences (Gaede et al., 2017). The function of this specialization is currently unknown; however, it is may be related to hovering flight (Altshuler & Srinivasan, 2018; Gaede et al., 2017). Ibbotson (2017) states that it may be due to the increased need to remain stable while feeding on nectar from flowers which may be moving in various directions due to environmental disturbances (Ibbotson, 2017). One goal of the current study is to confirm the population-level uniformity of direction preference in the LM of Anna's hummingbird.

Further studies investigating the response characteristics of the AOS presented drifting sine-wave gratings of varying temporal and spatial frequency to the contralateral eye while recording neural activity. Ibbotson (1994), in a study of the NOT and DTN in the wallaby, homologous to the LM in birds, conducted the first investigation of the spatiotemporal response characteristics of NOT-DTN neurons. He found there were two functional classes of cell: one cell type tuned to high temporal frequency (cycles/s) and low spatial frequency (cycles/degree), and another cell type tuned to low temporal frequency and high spatial frequency. Due to the relationship between velocity, temporal, and spatial frequency (velocity = TF/SF), these two cell types were referred to as "fast" and "slow" cells, respectively. Another important discovery was that NOT-DTN cells encode temporal frequency of motion rather than velocity (Ibbotson et al., 1994). Subsequent studies conducted in the pigeon found that the LM (Wylie & Crowder, 2000) and nBOR (Crowder

& Wylie, 2001) have very similar spatiotemporal response characteristics to the wallaby NOT-DTN. The peak velocity tuning of fast and slow cell classes of both species were strikingly similar for species of different taxonomic order. This may suggest similarities in the visual environment of distantly related taxa, which could have driven convergent evolution (Ibbotson & Price, 2001).

A key question is whether the spatiotemporal response characteristics of the visual system are conserved at the level of the LM or whether there is an area downstream of LM that is conserved. Because hummingbirds exhibit: 1) behavioural differences in visual guidance related to spatiotemporal features of the visual field, 2) anatomical differences including hypertrophy of the LM, a key optic flow responsive nucleus, and 3) neurophysiological differences in the population-level direction and speed preferences of the LM, does the hummingbird also exhibit spatiotemporal specialization in the LM that relates to its unique form of locomotion? To answer this question, I made electrophysiological recordings from the LM of hummingbirds and zebra finches. To test for direction preference, random dot fields were moved in 8 directions in 45° increments. Once the preferred direction was determined, drifting sinusoidal gratings of varying temporal and spatial frequency were presented in the preferred and anti-preferred direction. Each cell's spatiotemporal tuning was evaluated by fitting a 2-D Gaussian model to each peak in the spatiotemporal domain. Data collected from zebra finches and hummingbirds were then compared to previous pigeon data.

2. Research Chapter

2.1 Introduction

A moving animal experiences global visual motion across the retina, a signal known as optic flow, which is a key input for locomotor control (Dakin et al., 2016; Gibson, 1954, 1979; Goller & Altshuler, 2014). Optic flow sensing neurons have been identified in the midbrain of all vertebrate classes (Cochran et al., 1984; Gaede et al., 2017; Ibbotson et al., 1994; Hoffmann & Schoppmann, 1981; Manteuffel, 1982; Mustari & Fuchs, 1990; Simpson, 1984; Wylie & Crowder, 2000). These cells respond to large field visual motion, exhibit increased spiking activity in response to visual motion presented in a preferred direction, and suppression of activity in response to motion in the opposite (anti-preferred or null) direction. In birds, optic flow neurons are found in two midbrain nuclei: the nucleus of the basal optic root (nBOR) and the pretectal nucleus lentiformis mesencephali (LM) (Gaede et al., 2017; Wylie & Crowder, 2000), which are homologous to the mammalian nucleus of the optic tract (NOT) and the medial and lateral terminal nuclei, respectively (Fite, 1985; Ibbotson et al., 1994; McKenna & Wallman, 1985). Visual guidance of animal locomotion has been examined in a diversity of species, which has revealed control algorithms based on a variety of visual signals including image velocity, temporal frequency, and size of visual features (Baird et al., 2005; Borst & Euler, 2011; Dakin et al., 2016; Fry et al., 2009). However, how optic flow neurons encode these specific visual signals is not well understood in vertebrates.

One clue as to the relationship between locomotor strategies and visual neurons is provided by work on wallabies. Ibbotson et al. (1994) found that optic flow sensitive neurons in the NOT exist as two distinct functional cell-types (Ibbotson et al., 1994). One class of cell exhibits peak response to sinusoidal gratings of high temporal frequency and low spatial frequency whereas the

other class of cell responds maximally to low temporal and high spatial frequency. Because image velocity is the ratio of temporal to spatial frequency, these cell types are labelled “fast” and “slow” cells, respectively. Ibbotson et al. also reported that all NOT neurons in the wallaby were “tuned” to temporal frequency as opposed to spatial frequency or velocity. This means that over a range of spatial frequencies, the cells consistently responded to the same temporal frequency and were therefore temporal frequency tuned. Subsequent measurements from the LM (Wylie & Crowder, 2000) and nBOR (Crowder & Wylie, 2001) of pigeons yielded very similar spatiotemporal response characteristics to the wallaby. The peak velocity tuning of fast and slow cell classes of both species were strikingly similar for animals of a different taxonomic order. The “fast” pigeon cells were tuned to temporal frequency just as Ibbotson found in the wallaby. In contrast, the “slow” cells were typically tuned to the velocity of the stimulus. The discovery of functional classes of neurons which are specialized to encode different aspects of the visual scene suggest a relationship between visual neurons and different aspects of locomotion. Here we ask whether animals specialized for different modes of locomotion exhibit spatiotemporal specializations in optic flow neurons that may be related to their form of locomotion.

Birds are a good model organism to study the relationship between locomotor behaviour and optic flow neurons because they have enlarged eyes and associated visual structures (i.e., cerebellum, optic tectum), relative to brain size, and exhibit a diversity of locomotor strategies (Butler & Hodos, 2005; Howland et al., 2004; Kiltie, 2000). Behavioural experiments in hummingbirds, for example, have demonstrated distinct visual guidance algorithms for controlling hovering versus forward flight (Dakin et al., 2016; Goller & Altshuler, 2014). There is also evidence to suggest that distinct visual guidance strategies are used by different bird species performing the same mode of flight. It is likely that budgerigars balance optic flow in either eye

to control lateral flight trajectory (Bhagavatula et al., 2011); however, in this study static sine-wave gratings of only one spatial frequency were presented on the walls of the flight tunnel to provide optic flow input. Similar studies in hummingbirds using sine-wave gratings of many spatial frequencies found that hummingbirds do not respond to the same spatial frequency as budgies do and are tuned to a smaller bar width (Dakin et al., 2016). Additional experiments by Dakin et al. (2016) suggest that hummingbirds control lateral trajectory using the vertical rate of expansion of visual features. These distinct visual guidance algorithms observed in different species for the same flight mode (forward flapping flight) likely reflect an underlying difference in the spatiotemporal tuning of motion sensitive neurons. A key question is where in the visual system do these neurophysiological differences exist. Can specializations be observed at the level of the optic flow sensitive neurons in LM, or do these differences exist upstream in the retina or possibly at a higher level of integration? To date, only one electrophysiological study has recorded response properties of hummingbird LM neurons. Gaede et al. (Gaede et al., 2017) compared the direction and speed tuning of neurons in the LM to random dot fields and found that the hummingbird LM neurons are tuned to higher stimulus velocities as compared to zebra finches and pigeons. Hummingbird LM neurons also exhibited unique direction preferences (Gaede et al., 2017). This supports the idea that the neurophysiology of LM is not conserved across species; however, dot field stimuli are not sufficient to fully understand the spatiotemporal response properties of LM neurons and thus, the specializations between bird species remain unknown.

Based upon the different spatial frequencies that hummingbirds and budgerigars use to guide lateral course control, known anatomical specializations in the hummingbird including hypertrophy of the LM (Iwaniuk & Wylie, 2007), a key optic flow responsive nucleus, and the neurophysiological differences in the population-level direction and speed preferences of the

hummingbird LM, we hypothesized that *the hummingbird will exhibit spatiotemporal tuning specialization in the LM that relate to its unique form of locomotion.*

To explore the question of whether hummingbirds exhibit spatiotemporal tuning specializations in LM, we made extracellular electrophysiological recordings from the LM of hummingbirds and zebra finches while presenting stimuli to the contralateral eye. To test for direction preference, random dot fields were moved in 8 directions in 45° increments. Once the preferred direction of a cell was determined, drifting sinusoidal gratings of varying temporal and spatial frequency were presented in the cell's preferred and anti-preferred direction. Each cell's spatiotemporal tuning was evaluated by fitting a 2D Gaussian function to spatiotemporal contour plots. Data collected from zebra finches and hummingbirds were then compared to previous pigeon data.

2.2 Methods

2.2.1 Animals

Nine adult male zebra finches (*Taeniopygia guttata*) were obtained from Eastern Bird Supplies (Quebec, Canada). Seven adult male Anna's hummingbirds (*Calypte anna*) were caught on the University of British Columbia campus between September 2017 and March 2018. The number of individuals in the sample was determined by an a priori minimum cell sample of approximately 60-100 cells from each species. Zebra finches were housed in cages with 2-10 individuals and fed premium seed daily. Hummingbirds were housed individually in cages and fed twice daily with Nektar-Plus (Nekton, 13% by weight) and 30% sucrose solution. All experimental procedures were approved by the University of British Columbia Animal Care Committee in accordance with the guidelines set out by the Canadian Council on Animal Care (protocol number: A15-0116).

2.2.2 Surgery

Animals were anesthetized using a mixture of ketamine and xylazine (65 mg/kg ketamine and 8 mg/kg xylazine) via intramuscular injection in the pectoralis muscles. Additional doses were administered to maintain a steady surgical plane. A subcutaneous injection of 0.9% saline solution was administered just prior to each surgery to provide additional fluids. After anesthesia took effect, birds were positioned in a stereotaxic apparatus (Herb Adams Engineering, Glendora, CA, USA) equipped with ear bars and an adjustable beak bar which accommodated both species. Positioning of the ear bars varied depending on the species. For zebra finches, the ear bars were firmly held against the otic process of the quadrate bone, which comprises the anterior portion of the external acoustic meatus. The stereotaxic atlas of the zebra finch brain was then used to estimate the coordinates of LM (Konishi, unpublished). For hummingbirds, the ear bars were inserted into the opening of the external auditory meatus and coordinates were calculated using previous Nissl stained brain sections. Using the calculated coordinates, exposures approximately 1-2 mm in diameter were made in the skull over the telencephalon of the right hemisphere and sufficient dura mater was removed to expose the surface of the brain and allow access to LM in the vertical dimension.

2.2.3 Electrophysiology

Extracellular recordings were obtained in anesthetized birds using glass micropipettes containing 2M NaCl solution and with inner tip diameters ranging from 4-6µm. Electrodes were positioned in the x-y plane using manual micromanipulators and moved in the z-axis using an MC-5B single-axis Micro-Positioning Controller (National Aperture Inc., Salem, NH, USA) to drive a Motorized MicroMini™ Stage (MM-3M-F, (National Aperture Inc., Salem, NH, USA) mounted to the stereotaxic device. The analog signal supplied by cellular voltage changes was amplified

(×10,000; A-M Systems, Inc., Model 3000 differential amplifier; Sequim, WA, USA), band pass filtered from 0.1 – 3 kHz, and sampled at a rate of 30kHz. The analog signal was converted to a digital signal with a Micro1401-3 data acquisition unit (Cambridge Electronic Design Limited; Cambridge, UK) and recorded using Spike2 software for Windows (Cambridge Electronic Design Limited; Cambridge, UK). The computer running the visual stimulus was programmed to send a Transient-Transistor Logic (TTL) pulse that was received in a parallel channel by the Micro1401-3 data acquisition unit and then transferred to the recording computer to indicate each change in the stimulus program.

2.2.4 Visual Stimulus Presentation

Neurons in the LM are characterized by high spontaneous rates of activity and their preference for a direction of visual motion. To isolate and record individual cells, a hand-held stimulus (white bristol board with random black pattern) was moved in the four cardinal directions in the contralateral visual field. If a directional response was observed at a site, the stimulus monitor was placed 30 cm from the contralateral eye and parallel to the length of the bird. If a receptive field was observed to be dorsal or ventral the monitor was adjusted accordingly while maintaining the 30cm distance. All visual stimuli were presented on a 24-inch LED monitor (ASUS VG248QE) at a resolution of 1920 × 1080 pixels and a refresh rate of 144Hz. The monitor occupied an 84° × 53° area of the bird's visual field.

To test the neurophysiological response properties of LM cells, three stimulus programs were created using Psychophysics Toolbox-3 in Matlab R2017a. The first stimulus program tested the direction preference of the cell(s) in the recording site. This was achieved by creating a single plane of randomly positioned black dots (2.1° diameter) against a white background. The dots were moved in eight directions, 45° apart beginning at the angle of the beak (0°) at a speed of

6.4°/s (4.12cm/s). Moving dot field stimuli were presented for 4s followed by a 4s pause with 4 replicates for each direction.

The second stimulus program tested the spatiotemporal response properties of LM neurons. Sinusoidal wave gratings of varying temporal and spatial frequency were presented in the preferred and anti-preferred directions and the order of their presentation was randomized. Each sweep consisted of 4s of motion followed by a 2s pause. The spatial frequencies or spatial wavelengths of presented gratings ranged from 0.0155 – 1 cycles/degree of visual field (cpd) and temporal frequencies ranged from 0.031-16 cycles/second (Hz), which provided 42 unique sinewave grating treatments, each replicated 4 times. Spike rates were averaged over the 4 replicates for each of the 42 treatments to generate spatiotemporal contour plots in Matlab R2017a.

The final stimulus program tested the response of LM neurons to moving dot fields of varying visual motion coherence. Coherence in this context is defined as the percentage of dots in the dot field moving at the same speed and in the same direction. As in the first direction stimulus, a single plane of black dots on a white background were moved in the preferred and anti-preferred directions of each cell while the percent coherence was varied from 0-100% in 5% increments. A value of 0% coherence results in all dots moving in random directions at the same speed and 100% coherence results in all dots moving at the same speed and in the same direction. This provided 21 treatments which were presented in a random order and replicated 4 times. The stimulus program was modified later to testing the following coherence values: 0,20,40,80, and 100%. Each sweep consisted of 4s of motion followed by a 2s pause. Spike rates were averaged over the 4 replicates for each of the 21 treatments to generate response vs. coherence plots in Matlab R2017a.

2.2.5 Spike Sorting

Raw spike traces were sorted offline using Spike2 for Windows software and Matlab (R2014b and R2017a; MathWorks; Natick, MA, USA). Action potentials were extracted from the raw spike trace and categorized into spike templates created by setting two trigger thresholds in both the positive and negative voltage ranges to exclude noise and capture spikes. The templates encompassed the full spike length and for any spike to be added to a template, 60% of the points in a spike had to match the template. All similar templates were grouped using PCA cluster analysis and inspection of wave forms. The templates generated by sorting the first spike file were used to capture the same spikes in the other stimulus recordings. Sorted files were then exported to Matlab for further analysis.

2.2.6 Histology

At the end of each experiment, a small injection was made (Dextran Texas Red™ 3000MW, or Dextran micro-Emerald 3000MW, ThermoFisher Scientific) to confirm recording sites. Injections were made either manually or using iontophoresis (Digital Midgard Precision Current Source, Stoelting Co. Wood Dale, IL, USA) with a 4.5µA current for 7s ON/7s OFF cycles for 3-5 min and then allowed to diffuse from electrode tip for 5 min. Animals were administered a lethal dose of ketamine/xylazine mixture intramuscularly into the pectoralis muscles and immediately transcardially perfused with 0.9% saline followed by 4% paraformaldehyde.

Brains were extracted the following day and placed in 30% sucrose solution for cryoprotection until the brain sank in solution. Brains were then gel-blocked, placed into 4% PFA for 2 hours, and then transferred into 30% sucrose. Gel-blocked brains which sank in 30% solution

were then sectioned using a microtome (Model 860, American Optical) and mounted on slides for visualization of the injection site.

2.2.7 Directional analyses

Polar plots were generated for each isolated cell to determine directional tuning curve by fitting a B-spline function to the mean firing rates in each of the eight directions of motion. To determine whether a cell had a preferred direction of motion, a Rayleigh test was performed to test for uniformity. A cell was considered to have a preferred direction if its directional response was found to be non-uniform ($p < 0.05$). A mean direction vector was calculated for all cells with a non-uniform distribution using the following equation from Graham & Wylie, 2012:

$$Preferred\ direction = \ tan^{-1}\left(\frac{\Sigma_n(\mathrm{FR}_n \times \sin\theta_n)}{\Sigma_n(\mathrm{FR}_n \times \cos\theta_n)}\right)$$

where FR = firing rate (spikes/s); n = all eight directions of motion.

2.2.8 Analysis of Spatiotemporal Contour Plots

We generated contour plots illustrating the response of LM neurons to sine-wave gratings of varying temporal and spatial frequency. To determine the spatiotemporal tuning of LM cells, each cell's excitatory response plot was fitted with a variant of a 2D best-fit Gaussian function on logarithmic axes as used by Priebe et al., 2003.

$$G(sf, tf) = A \times e^{\frac{-(log_2(sf)-log_2(sf_o))^2}{{\sigma_{sf}}^2}} \times e^{\frac{-(log_2(tf)-log_2(tf_p(sf)))^2}{{\sigma_{tf}}^2}}$$

where

$$tf_p(sf) = \ 2^{(Q+1)\times\left(log_2(sf)-log_2(sf_0)\right)+\log_2(tf_0)}$$

where A is the amplitude of the Gaussian function in the z-axis, sf_0 and tf_0 are the peak values of the Gaussian function, sf and tf are the spatial and temporal frequency of a particular sine-wave grating, σ_{sf} and σ_{tf} are the spread of the Gaussian function in the spatial and temporal dimension, and Q is the slope of the relationship between preferred speed and spatial frequency. When Q is equal to 0, there is no relationship between the spatial frequency and the preference for speed. Thus, a plot of speed over spatial frequency would yield a slope of 0 and indicate speed tuning. When Q is equal to -1, there is a strong dependence of the speed preference on spatial frequency such that as spatial frequency increases by one log unit, the speed preference decreases by one log unit. In other words, the neurons tuning to spatial frequency and temporal frequency are independent.

Gaussian functions were fitted using the solver function in *Microsoft Excel*. The values of sf_0, tf_0, σ_{sf}, σ_{tf}, and Q were optimized to maximize the R^2 value between the Gaussian model fit (G values) and the real data (R values), which correspond to each of the sine-wave gratings tested in the matrix. This model was called the "unconstrained" model as the optimized variables are free to take on any value. Following Priebe et al., 2003, we used a method for classifying neurons as speed-tuned or spatiotemporally independent by fitting two additional Gaussian models; one speed-tuned, and one spatiotemporally independent model. In the speed-tuned model, the Q value was constrained to equal 0 which forces a speed-tuned prediction. In the spatiotemporally independent model, the Q value was constrained to equal -1 which forces a spatiotemporally independent prediction. We then assessed whether the actual tuning of the neuron was closer to the speed-tuned prediction or spatiotemporally independent prediction by computing the partial correlation of the real data with each of the simulated responses with the following equations:

$$R_{ind} = \frac{(r_i - r_s \times r_{is})}{\sqrt{(1 - {r_s}^2)(1 - {r_{is}}^2)}}$$

$$R_{speed} = \frac{(r_s - r_i \times r_{is})}{\sqrt{(1 - {r_i}^2)(1 - {r_{is}}^2)}}$$

where R_{ind} and R_{speed} are the partial correlations of the real data with the independent and speed-tuned models, r_i is the correlation of the real data with the independent prediction, r_s is the correlation of the real data with the speed-tuned prediction, and r_{is} is the correlation of the independent prediction with the speed-tuned prediction.

Following Winship et al., 2006, the statistical significance of R_{speed} and R_{ind} was calculated first with a Fisher Z-transform on the correlation coefficients:

$$Zf = 1/2 \times \ln\left(\frac{(1 + R)}{(1 - R)}\right)$$

where Zf is the z-score of R_{speed} or R_{ind}, and R is the corresponding partial correlation coefficient. The differences between the z-scores was then calculated using the following equation:

$$Z_{diff} = 1/2 \times \left(\frac{(Zf_{ind} - Zf_{speed})}{\left(\frac{1}{(N_{ind} - 3)}\right) + \left(\frac{1}{(N_s - 3)}\right)}\right)$$

where Zf_{ind} and Zf_{speed} are the Fisher Z-transform for R_{ind} and R_{speed}, and $N_{ind} = N_s$ = the number of sine-wave gratings used in the best-fit 2D Gaussian function. An absolute Z_{diff} of 1.65 corresponded to a p-value of 0.05 and was chosen to denote significance. The Z_{diff} was then used to classify cells into speed-tuned, independent, or unclassifiable. If $Z_{diff} \leq -1.65$ and $R_{speed} >> 0$, the cell was placed in the speed-tuned category. If $Z_{diff} \geq 1.65$ and $R_{ind} >> 0$, the cell was placed in

the spatiotemporally independent category. If $-1.65 < Z_{diff} < 1.65$, the cell was considered unclassifiable.

2.3 Results

We began by asking two questions: we first asked what the directional tuning properties were of hummingbird LM neurons and second whether hummingbirds exhibit directional tuning differences compared to zebra finches. Extracellular recordings were obtained from 88 LM neurons in 9 zebra finches and 98 LM nurons in 7 hummingbirds while presenting visual stimuli to the contralateral eye. During recording experiments, isolated cells were considered in LM if they exhibited directional responses to large field motion and had a spontaneous rate of activity. These characteristics distinguish LM neurons from neurons in surrounding visual structures, including the optic tectum and optic tract (Wylie & Frost, 1990). The one exception is omni-directional cells that comprised 11 (9 hummingbird and 2 zebra finch) of the 186 LM neurons recoded, which were excluded from the population level analysis as they did not exhibit a preferred direction of visual motion. The mean spontaneous rate was similar for both species (hummingbirds: 14.38 spikes/s ± 1.74 (SE), n=89; zebra finches: 13.24 ± 1.78 (SE), n=86).

2.3.1 Directional properties of LM neurons

A raw voltage trace of a representative forward-preferring hummingbird LM cell is shown in Fig 3A. This voltage trace shows responses to 8 directions of dot field motion, 45° apart over 1 minute. Spike sorting was used to identify single neurons in raw voltage traces and each action potential was converted to a time-event. The frequency of time-events (spikes) were used to construct peri-stimulus time histograms (PSTHs) of pooled data from 4 replications of each stimulus as shown in Fig 3B. Polar plots demonstrating directional tuning of single representative LM cells from each species are shown in Fig 3C-D. Rayleigh tests were applied to

each directional tuning curve to determine whether the cell's response was significantly non-uniform ($p < 0.05$). The Rayleigh test was used to determine whether a cell had a "preferred direction" of visual motion. If so, a mean direction vector was calculated as represented by the red lines in Fig 3C-D.

To determine population-level directional tuning, the preferred direction of each individual cell for both species was plotted in polar coordinates (Fig 3 E,F). This distribution was divided into 8 groups corresponding to the eight directions of presented motion for each species and summarized in Table 1. Most zebra finch cells (67%) preferred forward motion whereas a significant minority of hummingbird cells (42%) preferred forward motion. In addition to the cluster of forward preferring hummingbird cells, there was another large cluster of cells (22%) which preferred Down-Back motion (135°) as compared to zebra finches (12%). Apart from these two clusters of directional cells, all other directions are represented equally in the hummingbird whereas in the finch there are relatively few cells preferring back and down-forward.

Table 1. Distribution of direction preferences in LM. The 360° of motion was divided into eight sections of 45° centered about the directions in which visual motion was presented. The total number of cells for finches and hummingbirds were 86 and 89, respectively.

Species	*Forward*	*Down-Forward*	*Down*	*Down-Back*	*Back*	*Up-Back*	*Up*	*Up-Forward*
Zebra Finch	58 (67%)	0 (0%)	3 (3%)	10 (12%)	1 (1%)	6 (7%)	5 (6%)	3 (3%)
Hummingbird	37 (42%)	3 (3%)	7 (8%)	20 (22%)	9 (10%)	4 (4%)	3 (3%)	6 (7%)

The distribution of direction preferences found in hummingbirds confirms that hummingbirds indeed deviate from the pattern of all other vertebrates studied. However, the

uniformity found in this study was not quite to the degree that Gaede et al. (2017) found in a previous study of the directional response properties of the hummingbird LM.

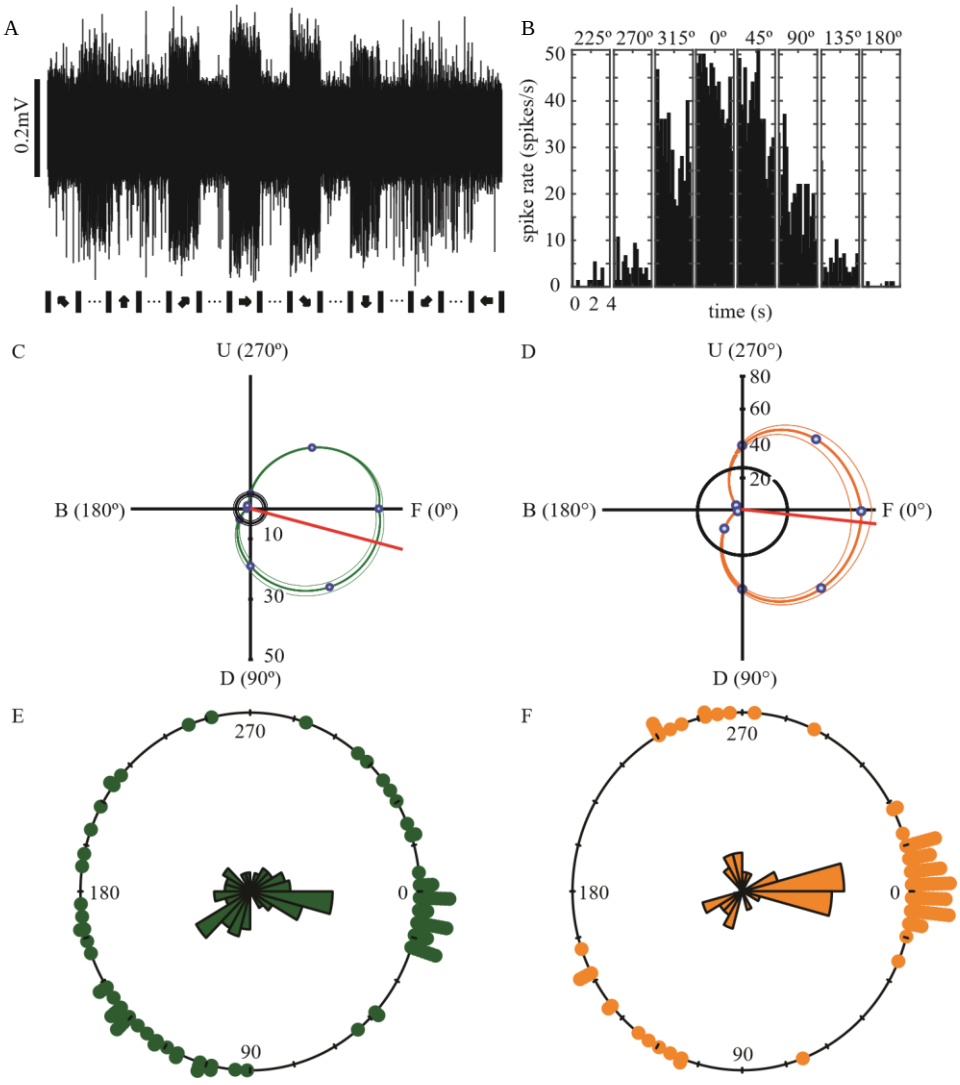

Figure 3. Directional analysis of LM cells in the hummingbird and zebra finch. A) A raw voltage trace of a representative hummingbird LM neuron in response to a random dot field stimulus. Arrows indicate the direction of dot field motion; three points in succession indicate pauses in stimulus motion, and vertical lines denote stimulus changes. B) Eight peristimulus time histograms corresponding to each of eight directions of dot field motion for the same cell as in A. Each histogram shows the average spike rate for four repetitions of the same stimulus divided into 200ms time-bins over 4s of stimulus motion. C) Polar plot showing the directional tuning of the cell in A. Mean firing rate (spikes/s) ± SE is shown to motion in each of eight directions (blue circles) with a B-spline fit to the points; black lines indicate spontaneous activity (spikes/s); red line indicates the preferred direction vector. F, forward motion (temporo-nasal); U, upward motion; B, backward motion (naso-temporal); D, downward motion. D) Polar plot as in C showing a representative zebra finch cell. E-F) Population-level direction analysis for all hummingbird cells (E, n = 89) and all zebra finch cells (F, n = 86). Rosette plots show the distribution of preferred directions of recorded neurons. Each point represents the preferred direction of an individual LM neuron.

2.3.2 Spatiotemporal Tuning Properties of LM Neurons

The results of the directional analysis confirmed that hummingbirds possess unique direction preferences in LM when compared to finches. We next asked whether the hummingbird LM also exhibited spatiotemporal tuning specializations in LM. Neural responses to an array of drifting sine-wave gratings were recorded from 79 zebra finch and 79 hummingbird LM cells. A small minority of neurons (4 zebra finch and 2 hummingbird) exhibited two peaks in the spatial domain. Each sine-wave grating presentation lead to a single histogram that was combined with all other sine-wave gratings presented to generate Fig 4A-B. Data gathered from the first hummingbird showed that some spatiotemporal peaks were at very low spatial frequencies and as a result, one more spatial frequency (0.0155cpd) was added to the stimulus program to bring the total spatiotemporal combinations to 42.

To illustrate tuning in the spatiotemporal domain, contour plots were generated for each cell in the preferred and anti-preferred direction (Fig. 4C-F). Temporal frequency (Hz) is plotted

on the y-axis, spatial frequency (cpd) is plotted on the x-axis, and on the z-axis is firing rate (spikes/s). Brighter colors on the contour plots correspond to greater magnitudes of excitation such that peaks are colored pale-yellow/white. Because motion in the preferred direction elicits excitation and motion in the anti-preferred direction elicits inhibition, these plots are referred to as excitatory (ER plots) and inhibitory response plots (IR plots), respectively, following Crowder et al. 2003. Figure 4C shows a representative hummingbird cell which exhibits a single peak in the spatiotemporal domain at 2Hz/0.031cpd. This cell is an example of temporally-tuned cell to a temporal frequency of 2Hz. This means that over a range of spatial frequencies (0.0155-0.125), this cell consistently responded to the same temporal frequency of 2Hz. The cell shown in Fig. 4D is a representative zebra finch cell also with one peak in the spatiotemporal domain at 2Hz/0.18cpd. The peak seen in this cell is oriented along a 45° angle or a slope of 1, which indicates velocity tuning. To ensure that a cell's activity to each sine-wave grating over the 4 replications was consistent, scatter plots were generated which show the variation (mean ± SE) of the cell's response (spikes/s) as a function of temporal frequency (Fig. 4G-H). Each scatter plot shows a cell's response to one spatial frequency over all temporal frequencies as indicated above each plot.

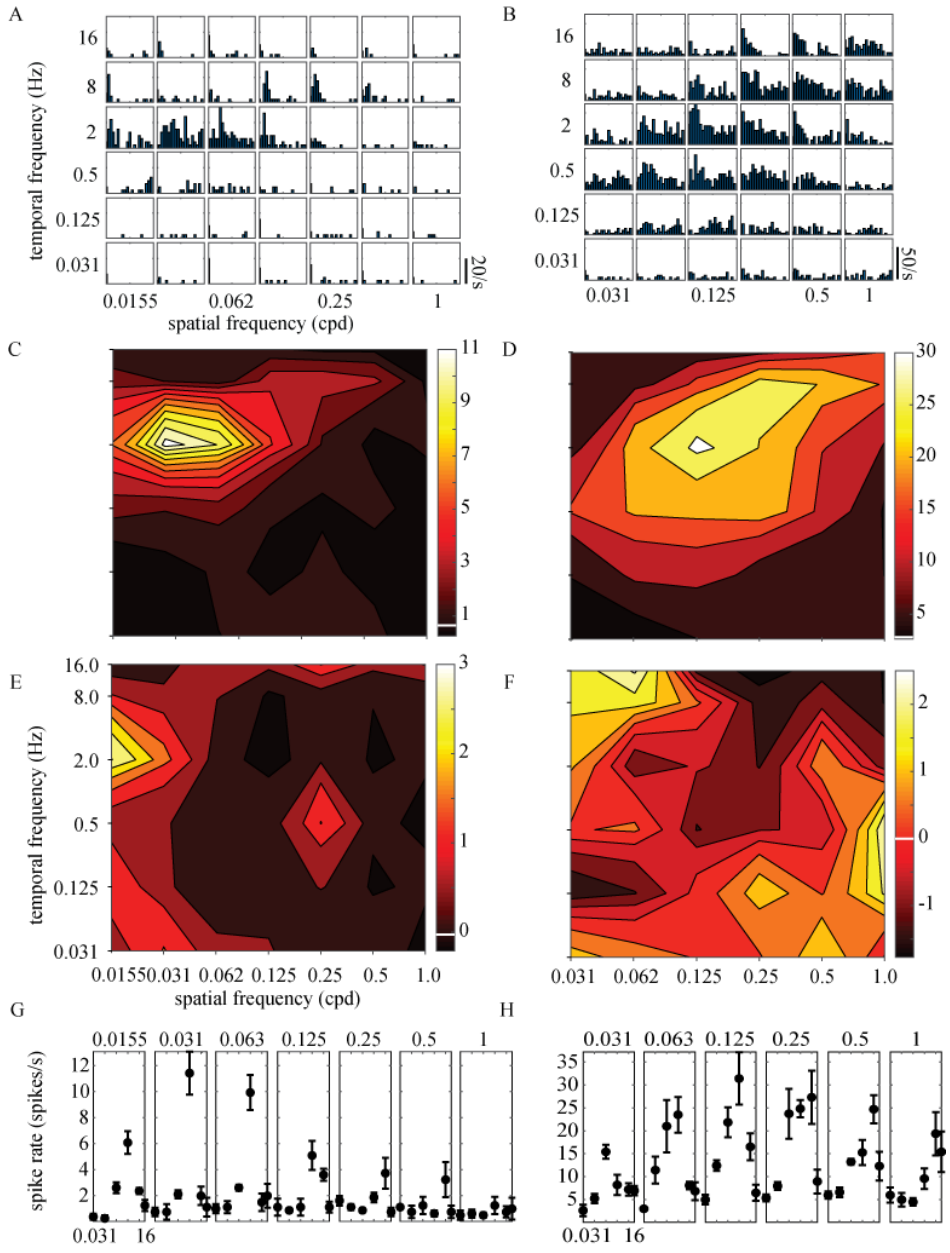
A
B
C
D
E
F
G
H
temporal frequency (Hz)
spatial frequency (cpd)
20/s
50/s
spike rate (spikes/s)

Figure 4. Spatiotemporal response properties of single LM units. A-B) Peristimulus time histograms showing responses of a representative hummingbird (A) and zebra finch (B) LM neuron to drifting sine-wave gratings of varying temporal and spatial frequency. Each histogram shows the average spike rate for four repetitions of the same stimulus divided into 100ms time-bins over 2s of stimulus motion. Because the first hummingbird tested showed responses to low spatial frequencies, we tested the remaining birds with an additional spatial frequency at the low end of the spectrum resulting in 42 spatiotemporal combinations. C-D) Contour plots showing the spatiotemporal tuning of the hummingbird cell in A and the zebra finch cell in B to gratings moving in the cell's preferred direction. In the preferred direction the colormap scale corresponds to raw firing rate (spikes/s); white line on colormap scale indicates spontaneous rate of activity. E-F) Contour plots showing the spatiotemporal tuning of the hummingbird cell in A and the zebra finch cell in B to gratings moving in the cell's anti-preferred direction. Colormap scale corresponds to *relative* firing rate (spikes/s) relative to spontaneous rate represented by the white line. G-H) Scatter plots showing the average firing rate (spikes/s) over temporal frequency for the cells in A and B. Each plot represents a cell's response to a single spatial frequency over all temporal frequencies.

2.3.3 Quantitative Analysis of Spatiotemporal Contour Plots

After producing ER and IR plots for each cell, we sought to determine where in the spatiotemporal domain each cell exhibited its peak response(s) and to what aspect of visual motion was each cell tuned (temporal frequency, spatial frequency, or velocity). The stimulus velocity (degrees per second; °/s) is the ratio of temporal to spatial frequency (velocity = TF/SF). Therefore, a peak in the spatiotemporal domain elongated along a line with a slope of 1 is tuned to velocity. A peak oriented along a vertical or horizontal line is spatially or temporally tuned, respectively. The cell in Fig. 5A is an example of a cell tuned to a velocity of ~7.5°/s. To quantitatively test whether a cell is tuned to velocity or is spatiotemporally independent, three Gaussian models (Fig 5B-D) were fitted to the real data (Fig 5A) as outline in section 2.2.8.

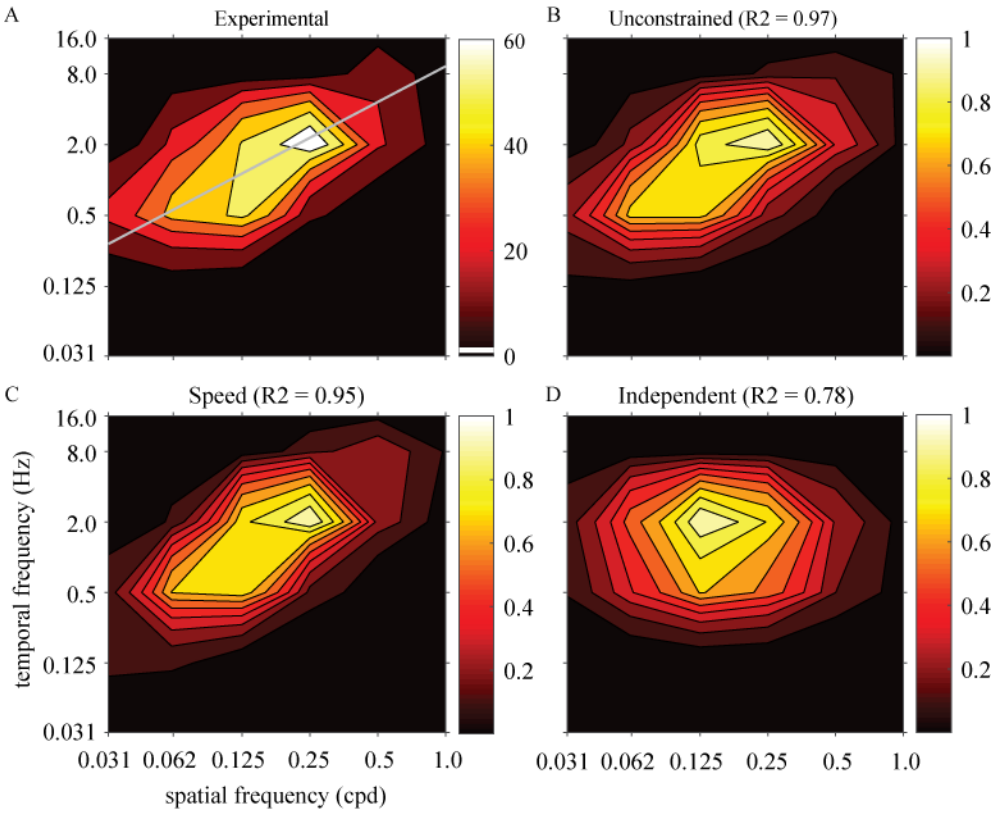

Figure 5. Method for determining spatiotemporal tuning. A) Spatiotemporal contour plot showing a velocity-tuned zebra finch LM neuron. Colormap scale represents raw firing rate (spikes/s); white line on colormap scale indicates spontaneous rate (spikes/s). The grey diagonal line represents a stimulus velocity of 7.5°/s. B) Unconstrained 2D Gaussian function fitted to the data in A. Colormap scale represents normalized firing rate (spikes/s). C) 2D Gaussian function fitted to the data in A showing the speed-tuned prediction (Q = 0). D) 2D Gaussian function fitted to the data in A showing the independent prediction (Q = -1). R squared plotted above the three fitted Gaussian functions were used to determine whether a cell was speed-tuned or spatiotemporally independent.

The peak values of all unconstrained 2D Gaussian model fits for hummingbirds, zebra finches, and previous pigeon data (Crowder et al., 2003) are presented in Fig 6A. The three species each have distinct peak distributions in the spatiotemporal domain. Hummingbird LM neurons were tuned to the fastest stimuli (87.7°/s ± 10.7; mean ± SE, see Fig 6B), which were generally of lower spatial frequency (0.09cpd ± 0.01; mean ± SE, see Fig 6C). The effect of species on both velocity ($p < 0.0001$) and spatial frequency ($p < 0.0001$) was significant whereas

the effect of species on temporal frequency (p = 0.086) was marginally insignificant (Fig 6D). A small number of hummingbird cells exhibited peak excitation at the lowest spatial frequency presented (0.0155cpd). This resulted in some of the Gaussian model fits appearing at least partly outside of the tested spatiotemporal space. Of the 8 hummingbird LM neurons that were tuned to slow stimuli, all but 1 preferred optic flow in the forward (temporal-to-nasal) direction, while the other cell preferred backward (nasal-to-temporal) motion. The location of 5 of these cells were mapped and 4 were found to be in LML. Of the 8 slow zebra finch cells, all preferred forward motion (temporal-to-nasal).

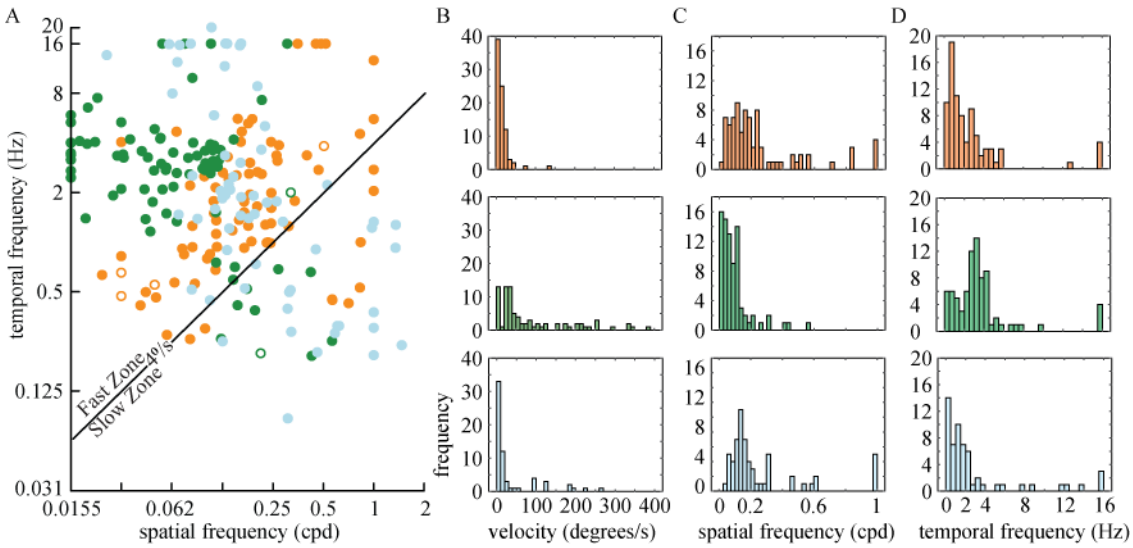

Figure 6. Hummingbird LM neurons prefer faster stimuli of lower spatial frequencies. A) Presented here are the locations of all best-fit 2D Gaussian peaks in the spatiotemporal domain. Each coloured circle represents the location (x,y) of the peak of each cell's unconstrained Gaussian model fitted to excitatory response plots. Dark green dots, orange dots, and light blue dots represent hummingbird, zebra finch, and pigeon data, respectively. Open circles represent the secondary peak only when a cell had more than one peak. Following Ibbotson (1994), the classification of fast and slow cells was based upon a cut-off of 4°/s represented by the diagonal line. B-D) Frequency histograms showing the velocity (B), spatial frequency (C), and temporal frequency (D) tuning distributions for all zebra finch (top), hummingbird (middle), and pigeon (bottom) cells.

The three Gaussian models (Fig. 5B-D) fitted to each spatiotemporal peak were then used to determine the partial correlation of the real data with the speed-tuned prediction (R_{speed}) and with the spatiotemporally independent prediction (R_{ind}), which are plotted against each other in Figure 7. The plot is divided into upper left-hand, lower right-hand and middle zones which represent a cell's classification as a speed-tuned, spatiotemporally independent, or unclassifiable cell, respectively. The previous pigeon data, when combined with the current data show that the three species exhibited substantial differences in the proportion of velocity-tuned neurons (upper left-hand zone), with pigeons having the fewest (9%) (not shown, see Fig 3A of Winship et al., 2006), zebra finches having the most (41%) and hummingbirds with an intermediate value (26%). In pigeons, only 'slow' cells (tuned to low temporal and high spatial frequency) are velocity-tuned, whereas both zebra finches and hummingbirds have a considerable number of 'fast' cells (tuned to high temporal and low spatial frequency) that are velocity-tuned. With respect to spatiotemporally independent LM neurons, pigeons and hummingbirds had a similar distribution (54% and 53%, respectively) while finches have significantly less independent neurons (23%).

As there was only a minimal number of slow cells found, the patterns mentioned above apply mainly to fast cells. When considering the slow cells, the finch cells were distributed uniformly throughout the three cell tuning classifications whereas hummingbird slow cells were found predominantly within the spatiotemporally independent category with none in the speed-tuned category.

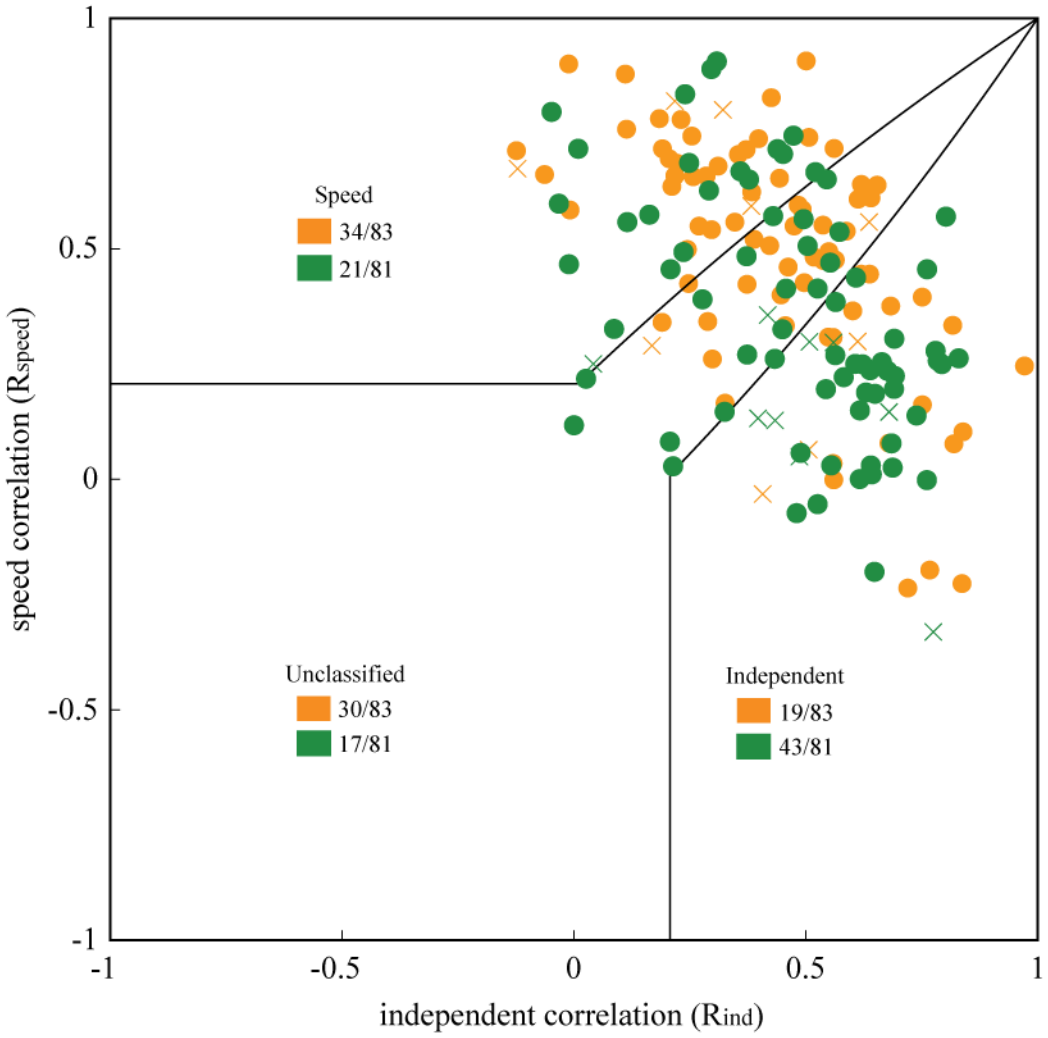

Figure 7. Hummingbird LM neurons are generally tuned to temporal frequency whereas zebra finch LM neurons are generally tuned to speed. Scatter plot showing the partial correlations of best-fit 2D Gaussian models with each of the predicted models: speed-tuned model (R_{speed}) or spatiotemporally independent model (R_{ind}). Each point indicates to which extent an LM neuron is speed-tuned or spatiotemporally independent. The plot is divided into three zones of cell classification by black lines which denotes the line of significance. Speed-tuned, unclassifiable, or spatiotemporally independent neurons fall into the upper left, middle, or lower right zones, respectively. Filled circles represent fast cells and cross markers represent slow cells.

2.3.4 Histological Confirmation of Recording Sites

To determine whether there was a relationship between where recordings were made within the hummingbird LM and the directional and spatiotemporal tuning, recording sites were mapped

within the midbrain (Fig 8). We were able to map 29 out of 49 total recording sites (59%) in 5 hummingbirds which accounted for 56 out of 89 total hummingbird LM cells (63%). We found that the population sample recorded in the hummingbird LM was greatly biased to cells found in the lateral subdivision of the nucleus, LML. Of the 29 mapped recording sites, 23 were found in LML which accounted for 45 of 56 cells of the mapped sites (80%), and 6 of the mapped recording sites were found in LMM/LPC which accounted for the remaining 11 of 56 cells (20%). Because of this biased sampling, and because the results of the current study are not in complete agreement with the findings of a previous study that explored the directional responses of hummingbird LM neurons (Gaede et al., 2017), we sought to determine whether there was directional topography within the hummingbird LM. We found that of the mapped cells recorded in LML, 21 of 45 cells preferred forward motion (47%) and of the cells in LMM there were 3 of 11 that preferred forward (27%). Although the sample size from LMM is small, this result supports the idea that there is directional topography in LM whereby the majority of forward cells are found within LML.

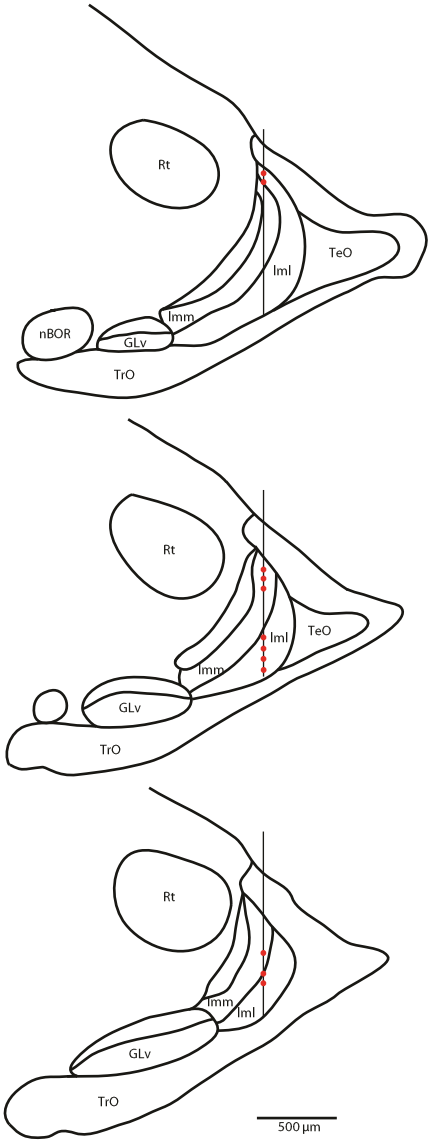

Figure 8. Most recordings in the hummingbird were made in the lateral subdivision of LM. Line drawings for three coronal brain sections, 80µm apart, from caudal (top) to rostral (bottom) showing contours of visual areas. Vertical lines represent electrode tracks and red dots on the line represent recording sites in LM.

2.4 Discussion

We hypothesized that based on the different spatial frequencies that hummingbirds and budgerigars use to guide lateral course control, there exist spatiotemporal tuning differences in the hummingbird LM. The LM is a visual area known to process optic flow related to self-motion, is

selectively hypertrophied in hummingbirds, and exhibits unique directional response properties in hummingbirds. We presented stimuli consisting of dot fields and drifting sinusoidal gratings of varying temporal and spatial frequency to anesthetized zebra finches and hummingbirds while recording in the contralateral LM. We also sought to confirm the uniformity of direction preferences found by Gaede et al. (2017) within the hummingbird LM. We found that hummingbirds do indeed exhibit unique directional response properties in LM (Fig 3). In addition, each of the three species considered exhibits distinct spatiotemporal tuning with respect to both the distributions of the peaks in the spatiotemporal landscape (Fig 6) and with respect to the tuning of LM cells to aspects of visual motion (spatial frequency, temporal frequency, and velocity) (Fig 7). Hummingbird LM neurons were tuned to the fastest stimuli, which were generally of lower spatial frequency. Of the few hummingbird LM neurons that were tuned to slow stimuli, all but one preferred optic flow in the forward (temporal-to-nasal) direction. Furthermore, 80% of the slow forward cells were found within LML. Hummingbirds and zebra finches, when compared with pigeons, exhibited substantial differences in the proportion of velocity-tuned neurons, with pigeons having the fewest (9%), zebra finches having the most (41%) and hummingbirds with an intermediate value (26%). In pigeons, only 'slow' cells are velocity tuned, whereas both zebra finches and hummingbirds have 'fast' cells that are velocity tuned. These species-specific differences are suggestive of neural specializations for different optic flow related behavior.

2.4.1 Directional Tuning

The ability of hummingbirds to sustain hovering flight to feed from flower nectar is unique among birds. This behaviour has been linked to the selective hypertrophy of the pretectal LM, which is known to be key in processing optic flow related to self-motion (Wylie & Crowder, 2000; Xiao & Frost, 2013). Gaede et al. (2017) discovered unique directional responses in the

hummingbird LM. We have confirmed the finding that the hummingbird is unique among vertebrates with respect to its direction preferences in LM; however, the distribution of direction preferences found in the current thesis is not "uniform" as was found by Gaede et al. We found that hummingbirds exhibit two large clusters of directional cells; one in the forward direction and one in the down-back direction (Fig 3). All other directions are equally represented (Table 1). This increased sensitivity to directions other than forward may be beneficial for the hummingbird during both stationary and translational hover (Goller & Altshuler, 2014; Ibbotson, 2017). Hummingbirds will often transition from flower to flower using a combination of hovering and slow flight that they can perform in all directions. These small positional adjustments during translational movements will produce optic flow signals processed by LM, which will drive gaze-stabilizing eye and head movements. The sensitivity to omnidirectional visual motion in LM would be beneficial in stabilizing the retinal image motion in the many directions that hummingbirds move while transitioning between flowers. During stationary hover while feeding, movement of the flower in any direction caused by wind, rain, or other disturbances will be readily processed by LM neurons and elicit motor compensation, thus allowing the bird to remain stable during stationary hover and feeding. The direction preference distribution observed in the current study however, was not as uniform as previously found (Gaede et al., 2017). We propose that the different observed results between studies of nearly identical methodology was due to biased anatomical sampling in the current study.

2.4.2 Anatomical Sampling Bias

We found that the distribution of recordings sites revealed a significant sampling bias where cells were mostly sampled from the LML (Fig 2.6). Many studies have looked at the directional responses of LM neurons in birds, only several of which have mapped recording sites (Winterson

& Brauth, 1985; Wylie & Crowder, 2000). Because LM data gathered in the pigeon was relatively consistent with respect to forward motion bias, there was little motivation to explore directional topography in LM. Wylie & Crowder (2000) were able to map 8 of 35 recording sites (23%) within the pigeon LM and found recordings to be equally distributed between LML and LMM. They found no differences between the two subdivisions with respect to direction preference or spatiotemporal properties. Winterson and Brauth (1985) conducted the best-known analysis of topography within LM. The researchers mapped 42 recording sites within LM, 13 in LML and 29 in LMM and found that the population-level direction preferences were reflected in both subdivisions. They also discovered retinotopy in LM whereby the dorsal aspect of LM contains cells with dorsally located receptive fields and as you move ventrally in LM the receptive fields correspondingly move ventrally. In the current study, we did not conduct a formal receptive field analysis, however we find the approximate locations of receptive fields in the LM are consistent with these findings. The only previous study looking at directional responses in hummingbird LM neurons was conducted by Gaede et al. 2017; however, a map of the recording sites made was not provided and we therefore cannot make a comparison of the samples taken between that study and the current study.

Our results indicate that there are significantly more forward preferring cells in the hummingbird LM than the study of Gaede et al., which leads to the question of to what degree this finding was due to anatomical sampling bias. Because we found that there was a much stronger bias toward forward motion in LML (47%) as compared to LMM (27%), we propose that the sampling bias is likely the reason for the difference in observed results. This would only apply however given that the sample taken by Gaede et al. was at least in part biased toward LMM. It is possible that the uniform distribution of direction preference found by Gaede et al. exists

primarily in LMM whereas LML follows the typical tetrapod pattern of forward motion bias. This difference motivates further study of the directional topography in LM in hummingbirds and indeed all birds as there is a lack of studies mapping recording sites.

2.4.3 Spatiotemporal Tuning

Previous pigeon studies showed that the LM contained mostly fast cells (66%) that were spatiotemporally independent, while the nBOR contained mostly slow cells (75%) tuned to velocity (Crowder et al., 2003; Winship et al., 2005). We found that both finch and hummingbird LM cells are almost exclusively in the "fast zone" and exhibit only a small group of cells in the slow zone, tuned to high spatial frequencies and low temporal frequencies. Our results are consistent with the fact that LM contains primarily fast cells; however, studies of the nBOR in both zebra finches and hummingbirds would need to be conducted to determine whether the nBOR contains an increased proportion of slow cells as compared to LM. Consistent with the findings of Gaede et al., the hummingbird LM neurons were tuned to significantly higher speeds as compared to finches (15.0°/s ± 1.9) or pigeons (44.6°/s ± 10.9) with a population average of 87.7°/s ± 10.7 (mean ± SE). Ibbotson (2017) suggested that the increased speed preference and the higher proportion of fast cells may be related to the fact that hummingbirds often fly close to flowers in dense vegetation (Ibbotson, 2017). Having neurons that encode global visual motion of higher velocities would be beneficial when flying near to visual features such as when hovering in front of a flower. This is because the closer one is to a visual feature, the higher the optic flow velocity of that feature for a given change in position.

Another explanation is provided by the dive displays known to be performed by Anna's hummingbirds. During these impressive displays, hummingbirds can reach average speeds of 27.3m/s, translating to 385 body lengths/s; the highest known length-specific velocity attained by

any vertebrate (Clark, 2009). While diving, hummingbirds need to maintain an awareness of where they are relative to the ground and surrounding objects otherwise the chance of collision is high. The increased sensitivity to fast motion may contribute to the hummingbird's ability to successfully perform these dives. It remains unknown whether the direction and speed preference differences exist only for Anna's hummingbird or whether the differences are generalized to all hummingbirds. Would other hummingbird species that don't perform dive displays exhibit the increased speed preference? This would allow us to determine whether the speed preference is related more to the courtship displays or more related to other factors such as hovering flight, a nectivorous feeding strategy, and the optic flow associated with these behaviours.

Hummingbirds are tuned to significantly lower spatial frequencies (0.09 ± 0.01) than either finches (0.25 ± 0.03) or pigeons (0.32 ± 0.04). Lower spatial frequencies correspond to sine-wave gratings composed of bars of greater width. In a natural scene this would correspond to coarse light intensity changes such as a tree trunk or a patch of flowers. When a hummingbird is flying through dense vegetation at high speeds, it doesn't seem likely that they would prioritize high spatial frequency stimuli. The fine detail of a leaf for example would be less important to visual guidance than the lower spatial frequency stimuli such as a tree or a patch of flowers nearby. The question becomes why pigeons and finches are tuned to higher spatial frequencies? It may relate to the need that pigeons and zebra finches must discriminate small objects, such as seeds, against a complex background. Picking out the correct seed-like object is more important to a pigeon or zebra finch than to a hummingbird that feeds primarily on nectar.

2.4.4 Function of Directional Topography

Interestingly, our results suggest that there is a directional topography within the hummingbird LM which has not been found in any other avian species studied (Winterson &

Brauth, 1985; Wylie & Crowder, 2000). The LMM is known to project to the oculomotor cerebellum, which is thought to be involved in flight control in cluttered environments while LML projects to the vestibulocerebellum, which is thought to control flight in open environments (Wylie et al., 2018). If the LMM-oculomotor cerebellum pathway is involved in controlling flight in cluttered environments, including hovering flight, one would expect that the LMM would be the location of uniform direction preference and higher speed preferences. Winterson and Brauth (1985) found that in pigeons the LMM prefers higher stimulus velocities than the LML. It was consequently suggested that the hypertrophy of LM in the hummingbird is mainly due to an expansion of LMM (Wylie et al., 2018). Conversely, the LML-vestibulocerebellar pathway controlling open flight would not have the sensitivity to all directions and would be tuned to slower speeds. Our results are partly consistent with this hypothesis because LMM has the more uniform distribution of direction preferences and LML contains the majority of slow forward cells. However, the mean velocity tuning of the mapped cells known to be in LML and LMM are 113.2 ± 17.2 and 50.9 ± 26.0 (mean ± SE), respectively, which is counter to the hypothesis. This large variation is likely due to the lack of sampling from LMM.

2.4.5 Conclusion

It was previously thought that the spatiotemporal response properties of the AOS and pretectum were conserved as previous measurements in wallabies and pigeons were found to be strikingly similar (Ibbotson et al., 1994; Ibbotson & Price, 2001; Crowder et al., 2003). Collectively, the current results indicate that this is not true. Every species considered in this study exhibited unique spatiotemporal tuning in the pretectal LM with hummingbirds having the most unique tuning. To determine whether this trend is true of all hummingbirds, further supporting the link between hovering flight and neural specialization, more hummingbird species need to be

considered. It is also important to ask whether these same differences occur in the nBOR of hummingbirds.

3. Conclusion

3.1 Optic Flow Analysis Across Species

Optic flow is a critical signal for navigation and locomotion in most animals. We know optic flow sensitive neurons exist in the brains of many vertebrates and have characterized their response properties (Cochran et al., 1984; Gaede et al., 2017; Ibbotson et al., 1994; Hoffmann & Schoppmann, 1981; Manteuffel, 1982; Mustari & Fuchs, 1990; Simpson, 1984; Wylie & Crowder, 2000); however, the question of how exactly optic flow is used to guide behaviour remains poorly understood. Moreover, the question remains whether the response properties of optic flow neurons are conserved across species. Therefore, this thesis examined the response properties of optic flow neurons in the LM to dot fields and sine-wave gratings of varying spatial and temporal frequency in both zebra finches and hummingbirds. Extracellular recordings were made in the LM of seven hummingbirds and nine zebra finches. The results of the current thesis suggest that the visual guidance of flight is more complex than previously thought. Due to the similar results found in studies of the wallaby NOT and the pigeon LM, Ibbotson and Price (2001) postulated that the similarities could represent a conserved system of ancient origin, or alternatively, could indicate similarities in the visual environment between the wallaby and pigeon (Ibbotson & Price, 2001). The current thesis contributes to our understanding of how the spatiotemporal tuning of visual neurons can vary between animals. The analysis of optic flow in the avian LM is specialized in different bird species and may not be as conserved as Ibbotson and Price proposed. Although this specialization has not been shown in the mammalian NOT, the observed variation is highly suggestive of neural specializations for optic flow analysis existing between mammals.

There are important limitations to consider however, when comparing only three species (Garland & Adolph, 1994) as was done in this thesis. It is difficult to generalize about adaptations

when you have such a small species sample. For a proper comparative study to be conducted many species would need to be considered with multiple representatives from each flight-mode as well as flightless birds. Although this would be useful in answering questions about the adaptations birds have to process their visual world, it would be a massive undertaking. With these limitations in mind, several hypotheses can be generated as a result of the current thesis.

There is a complex interplay between the environment an animal inhabits, its locomotor velocity, and its optic flow neurons. Depending whether an animal typically flies in open environments, such as soaring birds of prey, or cluttered environments such as hummingbirds, a very different optic flow environment is experienced. One might hypothesize that because moving in open environments creates lower velocity optic flow on average, the neurons responsible for processing optic flow would be tuned to lower velocities. Conversely, an animal occupying a dense forest with many obstacles to navigate will experience higher optic flow velocities on average and might accordingly require high velocity tuned optic flow neurons. In addition to the environment an animal inhabits, what might the velocity at which an animal moves contributes to optic flow analysis? An animal moving slowly in a dense forest might experience the same optic flow velocities as a very fast-moving animal, such as a peregrine falcon, in an open environment. What about migratory birds and birds that live in both open and cluttered environments? We do not have a complete picture yet; however, we now know that specializations do exist, and we can begin to ask where in the bird lineage do other specialists exist.

The studies of Ibbotson et al. (1994) and Wylie & Crowder (2000) did however find that the spatiotemporal tuning of the wallaby NOT and pigeon LM neurons was quite similar. This is interesting considering that pigeons have a much higher maximum movement speed (up to 18.9 m/s) compared to wallabies (6.3 m/s) and presumably a unique optic flow environment due to

flight ability (Biewener & Baudinette, 1995; Li et al., 2016). The only significant difference between the tuning of LM neurons in the pigeons versus NOT neurons in the wallaby were the presence of velocity-tuned neurons in the pigeon. Why would the pigeon need velocity-tuned neurons at the level of the LM and not the wallaby? Could it be that the reason for velocity-tuned neurons is the high speed at which the pigeon moves? Zebra finches and hummingbirds also move at high velocities (14 m/s and 27.3 m/s, respectively) and exhibit velocity-tuned neurons at the level of LM (Clark, 2009; Tobalske et al., 1999). Given that this is true, considering a turkey or chicken might reveal a lack of velocity-tuned neurons. Measurements made in fast moving or flying mammals would be informative here. One might ask whether in bats that can fly at speeds up of 14.2 m/s, exhibit velocity tuning in the NOT (Bullen et al., 2016).

Velocity-tuned cells could be found anywhere in the visual system. Why in birds is it at the level of the LM? Mammals are known to have velocity-tuned neurons in the middle temporal area, medial superior temporal area, and V1 (Bradley & Goyal, 2008; Duijnhouwer et al., 2013; Priebe et al., 2003; Rodman & Albright, 1987) but not in the NOT (Ibbotson et al., 1994). Why are velocity-tuned neurons primarily found in the mammalian cortex whereas they remain upstream in the avian LM? One explanation relates to what regions of the brain are enlarged in birds and mammals that provide the neural "real-estate" required to process visual signals. Mammals tend to have an enlarged cerebrum whereas birds typically have an enlarged midbrain. The increased processing power afforded by the enlargement of the cerebrum might have provided a selection pressure to shift the function of velocity sensitivity to later in the visual pathway. Conversely, the function of velocity extraction in birds must have been performed by other brain regions that were available at that point in evolutionary history such as the ancient midbrain because the avian cerebrum was not as well developed. Another explanation could be that extraction of velocity

earlier in the visual pathway might allow more time for the integration of these signals downstream of LM. The more rapid processing of optic flow into a velocity signal would be beneficial for birds avoiding high-speed collisions in cluttered environments. The earlier processing could have been driven by the vulnerability of birds that move at typically higher speeds than mammals and have a delicate skeleton.

3.2 Directional Topography

Another key question is whether the directional topography supported by the histological analysis of recording sites in the current thesis is correct. There has been only one systematic mapping of the LM in any bird carried out by Winterson and Brauth (1985). This study used tungsten microelectrodes where current can be injected into the brain, burning a small amount of tissue and creating a microlesion. It would be useful to conduct a similar study where the main objective is to map the directional topography of LM in the hummingbird or zebra finch or even to revisit this question in the pigeon with the most current methods. As the process of creating microlesions or making microinjections within the LM and mapping recording sites is quite tedious, it would be a worthwhile endeavor to develop calcium imaging protocols for this purpose. There are already such developments being used in mice (Lecoq et al., 2014) which use a multiple micro-endoscope apparatus to visualize multiple cortical areas simultaneously. Moreover, *in-vivo* calcium imaging methods are now being utilized in mouse models (Gulati et al., 2017). Calcium imaging provides huge benefits to electrophysiology as it couples anatomy and physiology directly and allows for the visualization of potentially many cells in multiple regions at once. This is especially useful because a neuron can make thousands of connections with other neurons in relatively distant locations (Hawkins & Ahmad, 2016). Indeed an LM neuron can receive inhibitory inputs from nBOR (Crowder et al., 2003), excitatory and inhibitory inputs from the

visual wulst (Crowder et al., 2004) as well as many other projections from the ventral thalamic nuclei, the midbrain, medulla, and cortex (for review see Pakan et al., 2006). To truly understand the function of LM in flight, *in vivo* recordings in awake and behaving birds must be made from arrays of neurons in LM as well as areas projecting to LM and areas that LM projects to.

Calcium imaging however does not come without difficulties when considering avian models. One major difficulty for calcium imaging in birds is the lack of transgenic lines which contain the means to express intracellular calcium sensors. However, there are promising developments in the Mooney lab at Duke which were recently able to express calcium indicators in targeted brain regions using CRE-dependent expression in zebra finches (Roberts et al., 2017). Using calcium imaging, the mapping of the LM can be done more rapidly and more accurately and potentially *in-vivo* to ask several questions. Firstly, whether the directional topography found in the hummingbird LM is real. Second, whether this trait is specific to Anna's hummingbird, hummingbirds in general, or a trait exhibited even by transiently hovering species. Lastly, with *in-vivo* calcium imaging, we can determine how neural activity in optic flow neurons is modulated *during* flight.

3.3 Future Electrophysiology Experiments

The connectivity and functionality of the LM and nBOR are similar in pigeons (Winterson & Brauth, 1985; Wylie & Frost, 1990; Wylie, 2001, for review see Wylie et al., 2018). One major difference is the population-level direction tuning. Because the LM in hummingbirds is so unique, a next logical step would be to ask what the direction, speed, and spatiotemporal response properties are of the hummingbird nBOR. Recent experiments conducted by Dr. Andrea Gaede and myself have been carried out in the Altshuler lab to explore this question. Measurements from the nBOR of both zebra finches and hummingbirds were made while presenting dot fields to the

contralateral eye. Both the directional tuning and speed tuning were assessed. From preliminary data, it seems that the nBOR follows a similar pattern to the pigeon nBOR (Wylie & Frost, 1990). This is not unexpected as the nBOR of the hummingbird was not anatomically enlarged when compared to other transiently hovering and non-hovering species (Iwaniuk & Wylie, 2007). If the hummingbird nBOR is confirmed to be similar to the pigeon nBOR, then both optic flow sensitive regions in the hummingbird exhibit a preference for multiple directions of motion. The nBOR exhibits up, down, and backward preferring cells in equal proportion with forward cells being rare. Evolutionary pressures to increase the optic flow sensitivity in the hummingbird seem to have driven the shift in direction preferences in the LM potentially because of its forward motion bias. Conversely, because nBOR already represented three directions of motion equally, there was potentially less pressure for this nucleus to shift its direction preferences.

3.4 Future Behavioural Experiments

Only a hand-full of behavioural studies have explored the role of optic flow in guiding avian flight (Bhagavatula et al., 2011; Dakin et al., 2016; Schiffner & Srinivasan, 2015; Schiffner et al., 2014). As the previously mentioned calcium imaging methods are advancing, virtual reality tunnel technology is concurrently advancing rapidly. Closed-loop behavioural systems which already exist at the small scale for insects and zebra fish (Stowers et al., 2017), will soon be able to accommodate birds. This will provide an interactive virtual reality where the stimulus presented depends on the animal's orientation and location. These closed-loop systems will be very powerful in answering questions about how optic flow and other visual signals guide behaviour. In addition, extremely lightweight (170 mg) systems for recording brain activity *in-vivo* have been developed by Neurotek as a part of the current thesis. Thanks to these recent advancements, we have the tools to record from the brain of flying birds that weigh as low as 4 grams. Nevertheless, sound

experimental protocols and effective animal training will need to be perfected to put these tools into practice.

3.5 Applications

Understanding visual algorithms used by animals to control flight can inform the visual guidance of artificial intelligence systems. For example, the correlation or Reichardt detector model that was originally developed as a result of work on the *Chlorophanus* beetle (*Chlorophanus* viridis) (Reichardt, 1957) has been used in robot visual guidance. This model provides a simple and effective way to extract motion and direction from the visual field (for review see Borst & Egelhaaf, 1989). Further work on the fly visual system has allowed for its implementation into an onboard motion detector circuit used in a fast obstacle-avoiding "robot mouche" (robofly) (Franceschini et al., 1992). The Reichardt model has more recently been implemented in the development of a visually-based autopilot system for a Micro Air Vehicle (Ruffier & Franceschini, 2003). This 100 g rotary craft can perform manoeuvres such as smooth cruise flight over planar ground and hill climbing using the analysis of optic flow. There have also been developments in the aquatic environment with autonomous underwater vehicles using the unique visual system of the box jellyfish as a model to navigate turbid environments (Song et al., 2017). As these systems become more complex, the usage of insect (or jellyfish) visual guidance may not be sufficient. Because of the low weight of an insect and therefore relatively low inertia, there is a much lower chance of permanent damage due to collision. For birds, obstacle avoidance is critical for survival. It has been shown that birds differ with respect to their visual guidance of flight speed and lateral course control (Dakin et al., 2016; Schiffner & Srinivasan, 2015), and therefore their mechanisms of obstacle avoidance could be of great use to the visual guidance of robot flight. The hummingbird

is of particular interest because of its heightened sensitivity to optic flow and its unique hovering behaviour.

Bibliography

Altshuler, D. L., & Srinivasan, M. V. (2018). Comparison of visually guided flight in insects and birds. *Frontiers in Neuroscience*, *12*(MAR). https://doi.org/10.3389/fnins.2018.00157

Baird, E., Srinivasan, M., Zhang, S., and Cowling, A. (2005). Visual control of flight speed in honeybees. *Journal of Experimental Biology*, *208*(20), 3895–3905. https://doi.org/10.1242/jeb.01818

Baron, J., Pinto, L., Dias, M. O., Lima, B., & Neuenschwander, S. (2007). Directional responses of visual wulst neurones to grating and plaid patterns in the awake owl, *26*(May), 1950–1968. https://doi.org/10.1111/j.1460-9568.2007.05783.x

Bhagavatula, P. S., Claudianos, C., Ibbotson, M. R., & Srinivasan, M. V. (2011). Optic flow cues guide flight in birds. *Current Biology*, *21*(21), 1794–1799. https://doi.org/10.1016/j.cub.2011.09.009

Biewener, A. a, & Baudinette, R. (1995). In vivo muscle force and elastic energy storage during steady-speed hopping of tammar wallabies (Macropus eugenii). *Journal of Experimental Biology*, *198*, 1829–41. Retrieved from http://jeb.biologists.org/content/198/9/1829.abstract

Borst, a, & Egelhaaf, M. (1989). Principles of visual motion detection. *Trends in Neurosciences*, *12*(8), 297–306. https://doi.org/10.1016/0166-2236(89)90010-6

Borst, A., & Euler, T. (2011). Seeing Things in Motion: Models, Circuits, and Mechanisms. *Neuron*, *71*(6), 974–994. https://doi.org/10.1016/j.neuron.2011.08.031

Bradley, D. C., & Goyal, M. S. (2008). Velocity computation in the primate visual system. *Nat Rev Neurosci.*, *9*, 686–695. https://doi.org/10.1097/OGX.0000000000000256.Prenatal

Bullen, R. D., McKenzie, N. L., & Cruz-Neto, A. P. (2016). Characteristic flight speeds in bats. *CEAS Aeronautical Journal*, *7*(4), 621–643. https://doi.org/10.1007/s13272-016-0212-5

Butler, A. B., & Hodos, W. (2005). *Comparative Vertebrate Neuroanatomy: Evolution and Adaptation* (2nd Editio). John Wiley & Sons Inc.

Chakravarthi, A., Kelber, A., Baird, E., & Dacke, M. (2017). High contrast sensitivity for visually guided flight control in bumblebees. *Journal of Comparative Physiology A*, *203*(12), 999–1006. https://doi.org/10.1007/s00359-017-1212-6

Clark, C. J. (2009). Courtship dives of Anna's hummingbird offer insights into flight performance limits. *Proceedings of the Royal Society B: Biological Sciences*, *276*(1670), 3047–3052. https://doi.org/10.1098/rspb.2009.0508

Cochran, S. L., Dieringer, N., & Precht, W. (1984). Basic Optokinetic-Ocular Reflex Pathways in the Frog. *The Journal of Neuroscience*, *4*(1), 43–57.

Collewijn, H. (1975). Oculomotor areas in the rabbit's midbrain and pretectum. *Journal of Neurobiology*, *6*(1), 3–22. https://doi.org/10.1002/neu.480060106

Collewijn, H. A. N. (1975). Direction-selective Units in the Rabbit's Nucleus of the Optic Tract. *Brain Research*, *100*, 489–508.

Crowder, N. A., Dawson, M. R. W., & Wylie, D. R. W. (2003). Temporal Frequency and Velocity-Like Tuning in the Pigeon Accessory Optic System. *Journal of Neurophysiology*, *90*(3), 1829–1841. https://doi.org/10.1152/jn.00654.2002

Crowder, N. A., & Wylie, D. R. (2001). Fast and slow neurons in the nucleus of the basal optic root in pigeons. *Neuroscience Letters*, *304*(3), 133–136. https://doi.org/10.1016/S0304-3940(01)01734-7

Dakin, R., Fellows, T. K., & Altshuler, D. L. (2016). Visual guidance of forward flight in hummingbirds reveals control based on image features instead of pattern velocity. *Proceedings of the National Academy of Sciences*, *113*(31), 8849–8854. https://doi.org/10.1073/pnas.1603221113

Duijnhouwer, J., Noest, A. J., Lankheet, M. J. M., van den Berg, A. V., & van Wezel, R. J. A. (2013). Speed and direction response profiles of neurons in macaque MT and MST show modest constraint line tuning. *Frontiers in Behavioral Neuroscience*, *7*(April), 1–11. https://doi.org/10.3389/fnbeh.2013.00022

Fite, K. V. (1985). Pretectal and Accessory-Optic Visual Nuclei of Fish, Amphibia and Reptiles: Theme and Variations. *Brain, Behavior and Evolution*, *26*, 71–90.

Franceschini, N., Pichon, J. M., & Blanes, C. (1992). From Insect Vision to Robot Vision. *Philosophical Transactions of the Royal Society B: Biological Sciences*, *337*, 283–294. https://doi.org/10.1098/rstb.1992.0106

Frost, B. J., Wylie, D. R., & Wang, Y. C. (1990). The processing of object and self-motion in the tectofugal and accessory optic pathways of birds. *Vision Research*, *30*(11), 1677–1688. https://doi.org/10.1016/0042-6989(90)90152-B

Fry, S. N., Rohrseitz, N., Straw, A. D., & Dickinson, M. H. (2009). Visual control of flight speed in Drosophila melanogaster. *Journal of Experimental Biology*, *212*(8), 1120–1130. https://doi.org/10.1242/jeb.020768

Gaede, A. H., Goller, B., Lam, J. P. M., Wylie, D. R., & Altshuler, D. L. (2017). Neurons Responsive to Global Visual Motion Have Unique Tuning Properties in Hummingbirds. *Current Biology*, *27*(2), 279–285. https://doi.org/10.1016/j.cub.2016.11.041

Gamlin, P. D. R. (2006). The pretectum : connections and oculomotor-related roles, *151*, 379–405. https://doi.org/10.1016/S0079-6123(05)51012-4

Gamlin, P. D. R., & Cohen, D. H. (1988). Projections of the Retinorecipient Pretectal Nuclei in the Pigeon (Columba livia). *J Comp Neurol*, *269*, 18–46.

Garland, T., & Adolph, S. C. (1994). Why Not to Do Two-Species Comparative Studies: Limitations on Inferring Adaptation. *Physiological Zoology*, *67*(4), 797–828. https://doi.org/115

Gibson, J. J. (1954a). The visual perception of objective motion and subjective movement. *Psychological Review*, *61*(5), 304–314. https://doi.org/10.1037/h0061885

Gibson, J. J. (1954b). The visual perception of objective motion and subjective movement. *Psychological Review*, *61*(5), 304–314. https://doi.org/10.1037/h0061885

Gibson, J. J. (1979). *The Ecological Approach to Visual Perception*. Taylor & Francis Group. https://doi.org/10.1386/eme.12.3-4.181

Gioanni, H. (1988). Stabilizing gaze reflexes in the pigeon (Columba livia) - I. Horizontbal and vertical optokinetic eye (OKN) and head (OCR) reflexes. *Experimental Brain Research*, *69*(3), 567–582. https://doi.org/10.1007/BF00247310

Goller, B., & Altshuler, D. L. (2014). Hummingbirds control hovering flight by stabilizing visual motion. *Proceedings of the National Academy of Sciences*, *111*(51), 18375–18380. https://doi.org/10.1073/pnas.1415975111

Graham, D. J., & Wylie, D. R. (2012). Zebrin-Immunopositive and -Immunonegative Stripe Pairs Represent Functional Units in the Pigeon Vestibulocerebellum. *Journal of Neuroscience*, *32*(37), 12769–12779. https://doi.org/10.1523/JNEUROSCI.0197-12.2012

Gulati, S., Cao, V. Y., & Otte, S. (2017). Multi-layer Cortical Ca Imaging in Freely Moving Mice with Prism Probes and Miniaturized Fluorescence Microscopy. *Journal of Visualized Experiments*, *124*(June), 1–9. https://doi.org/10.3791/55579

Hawkins, J., & Ahmad, S. (2016). Why Neurons Have Thousands of Synapses, a Theory of Sequence Memory in Neocortex. *Frontiers in Neural Circuits*, *10*(March), 1–13. https://doi.org/10.3389/fncir.2016.00023

Howland, H. C., Merola, S., & Basarab, J. R. (2004). The allometry and scaling of the size of vertebrate eyes. *Vision Research*, *44*(17), 2043–2065. https://doi.org/10.1016/j.visres.2004.03.023

Ibbotson, M. R. (2017). Visual Neuroscience: Unique Neural System for Flight Stabilization in Hummingbirds. *Current Biology*, *27*(2), R58–R61. https://doi.org/10.1016/j.cub.2016.11.052

Ibbotson, M. R., & Clifford, C. W. G. (2001). Interactions Between ON and OFF Signals in Directional Motion Detectors Feeding the NOT of the Wallaby. *J Neurophysiol*, *86*, 997–1005.

Ibbotson, M. R., Mark, R. F., & Maddess, T. L. (1994). Spatiotemporal response properties of direction-selective neurons in the nucleus of the optic tract and dorsal terminal nucleus of the wallaby, Macropus eugenii. *Journal of Neurophysiology*, *72*(6), 2927–2943.

Ibbotson, M. R., & Price, N. S. C. (2001). Spatiotemporal tuning of directional neurons in mammalian and avian pretectum: a comparison of physiological properties. *Journal of Neurophysiology*, *86*(5), 2621–4. Retrieved from http://www.ncbi.nlm.nih.gov/pubmed/11698548

Iwaniuk, A. N., & Wylie, D. R. W. (2007). Neural specialization for hovering in hummingbirds: Hypertrophy of the pretectal nucleus lentiformis mesencephali. *J Comp Neurol*, *500*(2), 211–221. https://doi.org/10.1002/cne

K. P. Hoffmann, & Schoppmann, A. (1981). A Quantitative Analysis of the Direction-specific Response of Neurons in the Cat's Nucleus of the Optic Tract. *Exp Brain Res*, *42*, 146–157.

Kiltie, R. A. (2000). Scaling of Visual Acuity with Body Size in Mammals and Birds. *Functional Ecology*, *14*(2), 226–234.

Lecoq, J., Savall, J., Vučinić, D., Grewe, B. F., Kim, H., Li, J. Z., … Schnitzer, M. J. (2014). Visualizing mammalian brain area interactions by dual-axis two-photon calcium imaging. *Nature Neuroscience*, *17*(12), 1825–1829. https://doi.org/10.1038/nn.3867

Li, Z., Courchamp, F., & Blumstein, D. T. (2016). Pigeons home faster through polluted air. *Scientific Reports*, *6*(December 2015), 1–6. https://doi.org/10.1038/srep18989

Manteuffel, G. (1982). The accessory optic system in the newt, Triturus cristatus: unitary response properties from the basal optic neuropil. *Brain, Behavior and Evolution*, *21*, 175–184.

McKenna, O. C., & Wallman, J. (1985). Accessory Optic System and Pretectum of Birds: Comparisons with those of other Vertebrates. *Brain, Behavior and Evolution*, *26*(2), 91–116.

Medina, L., & Reiner, A. (2000). Do birds possess homlogues of mammalian primary visual, somatosensory and motor cortices? *Trends in Neurosciences*, *23*(1), 1–12.

Mustari, M. J., & Fuchs, A. F. (1990). Discharge Patterns of Neurons in the Pretectal Nucleus of the Optic Tract (NOT) in the Behaving Primate. *J Neurophysiol*, *64*(1).

Pakan, J. M. P., Krueger, K., Kelcher, E., Cooper, S., Todd, K. G., & Wylie, D. R. W. (2006). Projections of the nucleus lentiformis mesencephali in pigeons (Columba livia): A comparison of the morphology and distribution of neurons with different efferent projections. *Journal of Comparative Neurology*, *495*(1), 84–99. https://doi.org/10.1002/cne.20855

Pettigrew, J. D. (1978). *Frontiers in Visual Science*. *Comparison of the Retinotopic Organization of the Visual Wulst in Nocturnal and Diurnal Raptors, with a Note on the Evolution of Frontal Vision* (2nd ed.). Berlin: Heidelberg: Springer.

Pettigrew, J. D., & Konishi, M. (1976). Neurons Selective for Orientation and Binocular Disparity in the Visual Wulst of the Barn Owl (Tyto alba). *Science*, *193*(4254), 675–678.

Portelli, G., Ruffier, F., & Franceschini, N. (2010). Honeybees change their height to restore their optic flow. *Journal of Comparative Physiology A: Neuroethology, Sensory, Neural, and Behavioral Physiology*, *196*(4), 307–313. https://doi.org/10.1007/s00359-010-0510-z

Priebe, N. J., Cassanello, C. R., & Lisberger, S. G. (2003). The neural representation of speed in macaque area MT/V5. *The Journal of Neuroscience*, *23*(13), 5650–5661.

https://doi.org/23/13/5650 [pii]

Reichardt, W. (1957). Autokorrelations-Auswertung als Funktionsprinzip des Zentralnervensystems. *Zeitschrift Für Naturforschung B*, *12*(7), 448–457.

Roberts, T. F., Hisey, E., Tanaka, M., Kearney, M. G., Chattree, G., Yang, C. F., … Mooney, R. (2017). Identification of a motor-to-auditory pathway important for vocal learning. *Nature Neuroscience*, *20*(7), 978–986. https://doi.org/10.1038/nn.4563

Rodman, H. R., & Albright, T. D. (1987). Coding of visual stimulus velocity in area MT of the macaque. *Vision Research*, *27*(12), 2035–2048. https://doi.org/10.1016/0042-6989(87)90118-0

Ruffier, F., & Franceschini, N. (2003). OCTAVE: a bioinspired visuo-motor control system for the guidance of micro-air-vehicles. *Proceedings of SPIE*, (April). https://doi.org/10.1117/12.498193

Scalia, F. (1972). The Termination of Retinal Axons in the Pretectal Region of Mammals. *Journal of Comparative Neurology*, *145*, 223–258.

Schiffner, I., & Srinivasan, M. V. (2015). Direct evidence for vision-based control of flight speed in budgerigars. *Scientific Reports*, *5*, 1–7. https://doi.org/10.1038/srep10992

Schiffner, I., & Srinivasan, M. V. (2016). Budgerigar flight in a varying environment: flight at distinct speeds? *Biology Letters*, *12*(6), 717–743. https://doi.org/10.1098/rsbl.2016.0221

Schiffner, I., Vo, H. D., Bhagavatula, P. S., & Srinivasan, M. V. (2014). Minding the gap: in-flight body awareness in birds. *Frontiers in Zoology*, *11*(1), 64. https://doi.org/10.1186/s12983-014-0064-y

Simpson, J. I. (1984). The accessory optic system. *Ann. Rev. Neurosci.*, *7*, 13–41.

Song, Z., Schwartz, E., & Mohseni, K. (2017). Bioinspired visual guidance in turbid underwater environment. *Proceedings of IEEE Sensors*. https://doi.org/10.1109/ICSENS.2017.8234184

Stowers, J. R., Hofbauer, M., Bastien, R., Griessner, J., Higgins, P., Farooqui, S., … Straw, A. D. (2017). Virtual reality for freely moving animals, *14*(10). https://doi.org/10.1038/nmeth.4399

Straw, A. D., Lee, S., & Dickinson, M. H. (2010). Visual control of altitude in flying drosophila. *Current Biology*, *20*(17), 1550–1556. https://doi.org/10.1016/j.cub.2010.07.025

Tobalske, B. W., Peacock, W., & Dial, K. P. (1999). Kinematics of flap-bounding flight in the zebra finch over a wide range of speeds. *The Journal of Experimental Biology*, *202*, 1725–1739. Retrieved from http://www.ncbi.nlm.nih.gov/pubmed/10359676

Vincze, O., Vágási, C. I., Pap, P. L., Osváth, G., & Møller, A. P. (2015). Brain regions associated with visual cues are important for bird migration. *Biology Letters*, *11*. https://doi.org/10.1098/rsbl.2015.0678

Wang, Y. C., Jiang, S., & Frost, B. J. (1993). Visual processing in pigeon nucleus rotundus:

Luminance, color, motion, and looming subdivisions. *Visual Neuroscience*, *10*(1), 21–30. https://doi.org/10.1017/S0952523800003199

Winship, I. R., Crowder, N. a, & Wylie, D. R. W. (2006). Quantitative reassessment of speed tuning in the accessory optic system and pretectum of pigeons. *Journal of Neurophysiology*, *95*(1), 546–551. https://doi.org/10.1152/jn.00921.2005

Winterson, B. J., & Brauth, S. E. (1985). Direction-selective single units in the nucleus lentiformis mesencephali of the pigeon (Columba livia). *Experimental Brain Research*, *60*(2), 215–226. https://doi.org/10.1007/BF00235916

Wylie, D. R., & Frost, B. J. (1990). The visual response properties of neurons in the nucleus of the basal optic root of the pigeon : a quantitative analysis. *Exp Brain Res*, *82*, 327–336.

Wylie, D. R., Gutiérrez-Ibáñez, C., Gaede, A. H., Altshuler, D. L., & Iwaniuk, A. N. (2018). Visual-cerebellar pathways and their roles in the control of avian flight. *Frontiers in Neuroscience*, *12*, 1–10. https://doi.org/10.3389/fnins.2018.00223

Wylie, D. R., Kolominsky, J., Graham, D. J., Lisney, T. J., & Gutierrez-Ibanez, C. (2014). Retinal projection to the pretectal nucleus lentiformis mesencephali in pigeons (Columba livia). *Journal of Comparative Neurology*, *522*(17), 3928–3942. https://doi.org/10.1002/cne.23649

Wylie, D. R. W. (2001). Projections from the nucleus of the basal optic root and nucleus lentiformis mesencephali to the inferior olive in pigeons (Columba livia). *Journal of Comparative Neurology*, *429*(3), 502–513. https://doi.org/10.1002/1096-9861(20010115)429:3<502::AID-CNE10>3.0.CO;2-E

Wylie, D. R. W., & Crowder, N. A. (2000). Spatiotemporal properties of fast and slow neurons in the pretectal nucleus lentiformis mesencephali in pigeons. *Journal of Neurophysiology*, *84*(5), 2529–2540.

Xiao, Q., & Frost, B. J. (2013). Motion parallax processing in pigeon (Columba livia) pretectal neurons. *European Journal of Neuroscience*, *37*(7), 1103–1111. https://doi.org/10.1111/ejn.12115